A Collagen Matrix Promotes Anti-Inflammatory Healing Macrophage Function through a miR-92a Mechanism

By

Zachary Lister

This thesis is submitted to the Faculty of Graduate and Postdoctoral Studies in partial fulfillment of the requirements for the Degree of:

Master of Science in Cellular and Molecular Medicine

Department of Cellular and Molecular Medicine
Faculty of Medicine
University of Ottawa
Division of Cardiac Surgery
University of Ottawa Heart Institute

Abstract

MicroRNAs are emerging as key players in the regulation of the post-myocardial infarction (MI) environment. We previously identified that matrix-treated hearts had down-regulated expression of miR-92a, a miRNA with inflammatory and migratory effects that is normally up-regulated after MI. We have shown that type I collagen matrix treatment at 3h post-MI leads to less inflammation and improved cardiac function, but the underlying mechanisms remain to be better characterized. The goal of this study was to elucidate a possible role of miR-92a in the anti-inflammatory/pro-wound healing effect of matrix treatment post-MI. C57BL/6J mice underwent LAD ligation to induce MI. Hearts were removed at 4h, 1d, 3d, and 7d post-MI and RNA was extracted from infarct and peri-infarct tissue. PCR analysis revealed that hearts injected with matrix at 3h post-MI resulted in significantly decreased miR-92a at 4h, 1d, and 3d compared to non-injected animals at each time point ($p<0.0001$) and PBS injected animals at 4h and 7d ($p<0.004$). Several targets of miR-92a and regulators of macrophage polarization were found to be up-regulated ($p<0.05$) early in MI indicating early amelioration of inflammatory processes. *In vitro*, macrophages cultured on matrix also had decreased expression of miR-92a compared to cultures on tissue culture poly styrene (TCPS) ($p<0.001$). Integrins α5 (ITGAα5) and αV (ITGAαV), involved in cell-matrix interactions, as well as inflammatory regulators S1PR1 and SIRT1 were identified as putative miR-92a targets. When miR-92a is over-expressed in macrophages, ITGα5 ($p=0.0002$), ITGαV ($p=0.02$), and S1Pr1 ($p<0.0001$), and SIRT1 ($p=0.03$) all had decreased expression. STAT3 and IL-10 were found to be moderately down-regulated. In evaluating macrophage phenotypes, M2 macrophages had reduced miR-92a expression on matrix compared to M1 macrophages. The migration of M2 macrophages into the matrix is increased compared to M1 macrophages. We report that the beneficial effects of matrix

treatment post-MI may be mediated, at least in part, through its ability to regulate miR-92a and pro-wound healing mechanisms in macrophages. These results present the matrix as a novel non-pharmacological approach to locally regulate miRNAs *in vivo* for reducing inflammation and protecting the myocardium post-MI.

Table of Contents

List of Figures

List of Tables

Abbreviations

3’ UTR	3’ Untranslated Region
ABCA1	ATP Binding Cassette
APS	Ammonium Persulfate
BSA	Bovine Serum Albumin
CAC	Circulating Angiogenic Cells
CAM	Cell Adhesion Molecule
CCL2	Chemokine (C-C motif) Ligand
CPC	Circulating Progenitor Cells
cTM	Cardiac Tissue Macrophage
CVD	Cardiovascular Disease
DAPI	4’,6-diamidino-2-phenolindole
DMEM	Dulbecco Modified Eagle Medium
ECM	Extracellular Matrix
EDC	1-Ethyl-3-(3-Dimethylaminopropyl) Carbodiimide
EDTA	Ethylenediaminetetraacetic Acid
GFP	Green Fluorescent Protein
FISH	Fluorescent In Situ Hybridization
HBSS	Hank’s Balanced Salt Solution
HDL	High Density Lipoprotein
HPRT	Hypoxanthine-guanine Phosphoribosyltransferase
IFN-γ	Interferon Gamma
iNOS	Inducible Nitric Oxide Synthase

ITG	Integrin
JAK	Janus Kinase
LAD	Left Anterior Descending
LNA	Locked Nucleic Acid
LPS	Lipopolysaccharide
LV	Left Ventricle
LVEF	Left Ventricular Ejection Fraction
M-CSF	Macrophage Colony Stimulating Factor
MeOH	Methanol
MES	2(-N-Morpholino) Ethanesulfonic Acid
MI	Myocardial Infarction
miRNA/miR	MicroRNA
MLKL	Mixed Lineage Kinase Domain-like
MMP	Matrix Metalloproteinase
NHS	N-Hydroxysuccinimide
PAGE	Polyacrylamide Electrophoresis Gel
PBS	Phosphate Buffered Saline
PCL	Poly(ε-caprolacetone)
PDO	Polydioxanone
PFA	Paraffin Aldehyde
PKD	Polycystic Kidney Disease
p-STAT3	Phosphorylated-STAT3
PTEN	Phosphate and Tension Homologue

RECK	Reversion Inducing Cysteine Rich Protein with Kazal Motifs
RIN	RNA Integrity Number
RIP	Receptor Interacting Protein
RISC	RNA Induced Silencing Complex
ROS	Reactive Oxygen Species
RT	Reverse Tracription
RT-qPCR	Real Time Quantitative Polymer Chain Reaction
S1Pr1	Sphingosine-1-Phosphate Receptor 1
SDS	Sodium Dodecyl Sulfate
SIRT1	Sirtuin-1
SIS-ECM	Small Intestinal Submucosal Extracellular Matrix
Spry1	Sprouty Homologue 1
STAT3	Signal Transducer and Activator of Transcription
STEMI	ST-elongated Myocardial Infarction
TCPS	Tissue Culture Polystyrene
TEMED	Tetramethyethylenediamine
TGF-β	Transforming Growth Factor Beta
TLR	Toll-like Receptor
TNF-α	Tumor Necrosis Factor Alpha
VEGF	Vascular Endothelial Growth Factor

Acknowledgements

My time at the University of Ottawa has been an incredible learning experience which would not have been possible without the help and guidance from so many people. To my supervisor, Dr. Erik Suuronen, thank you for taking me on and allowing me to pursue my Master's project under your supervision and providing me with guidance from day one.

To members of the Suuronen lab, namely, Brian McNeill, Nick Blackburn, and Bora Nadlacki; thank for all the help and countless laughs along the way from everyday lunches to wine tasting.

I would also like to thank my co-supervisor Dr. Katey Rayner whose incredible knowledge and guidance have be paramount in my success. Dr. Rayner, showed great dedication to research and constant availability to share her expertise which I found truly admirable.

The Rayner lab as a whole, Michele, MyAnh, Denuja, and Benoit, are some of the nicest people I have met who always made me feel included in lab activities and lunches despite being a part-time member. Their knowledge and expertise in inflammatory cells has been invaluable throughout my Master's.

I would like to extend my gratitude to my thesis advisory committee Dr. Marjorie Brand and Dr. Balwant Tuana for their time and note regarding my progress. They have provided me with valuable advice which helped strengthen the overall direction of the project.

A final thank you to friends and family who have helped me along the way. To Sarah Coakeley, you played a major role in the completion of my Master's through your continuing support, patience, and ability to make me laugh, smile, and motivate throughout the good and bad times. Also to the Coakeley family for taking me in on holidays in which I could not make it home, thank you for the love and laughs. I would also like to thank my good friends Mac, Court, and Bradley for always making me laugh and distracting me from work. I know none of this would have been possible without the love and support of my family. Last, but certainly not least, the biggest thank you to my parents Maria and Mark for standing by my decision to pursue my Master's even though it forced me to move so far away from home and to my brother Jordan, thanks for being you; you are a very special boy.

I know none of this would have been possible without any of you, for that; I thank you.

List of Contributions

Dr. Erik Suuronen and Dr. Katey Rayner were responsible for conceptualizing, designing and funding the project. Animal surgeries and injections were performed by Richard Seymour, with tissue collection assisted by Nick Blackburn. Technical training and support was provided by all members of the Suuronen and Rayner Labs.

Introduction

1. Introduction

1.1 Normal Cardiac Physiology

The primary function of the heart is to distribute oxygenated blood through the body for cellular respiration, nutrient distribution and waste removal. Cardiac muscle has a unique composition with qualities of both skeletal and smooth muscle. Similar to skeletal muscle, cardiac muscle is striated, however it is not under voluntary control giving it characteristics of smooth muscle as well. To support the very high metabolic activity of the heart, the myocardium is densely vascularized to ensure adequate oxygen metabolism to avoid metabolic stress and the formation of reactive oxygen species (ROS). Electrical communication between cardiomyocytes occurs via gap junctions and is critical for regulating synchronous muscle contractions and pumping function. Another key factor the myocardium relies on is the extracellular matrix (ECM) for mechanical support. During diastole, collagen in the ECM passively provides stiffness to prevent temporal dilation, while during systole it is able to transduce force across the myocardium (Leonard et al. 2012; Winslow et al. 2015). In addition, the interaction of cardiomyocytes with the ECM promotes survival and function (Kresh and Chopra, 2011; Okada et al., 2013). Although much of the cellular mass of the heart is composed of cardiomyocytes, there are also several other cell types, including endothelial cells, fibroblasts and macrophages which have support and maintenance roles crucial to cardiac function.

1.2 Myocardial Infarction and Cardiac Repair

Cardiovascular disease (CVD) is defined as a physiological condition that causes impaired function of the heart, or blood vessels of the circulatory system. Myocardial infarction (MI) is often the consequence of prolonged CVD and results from the blockage of one or more coronary arteries causing ischemia (lack of oxygen and nutrients due to loss of blood supply) to the myocardium (Frangogiannis, 2008; Rane and Christman, 2011). The ischemic event triggers a switch from aerobic to anaerobic respiration leading to acidosis from lactic acid accumulation, the generation of reactive oxygen species (ROS) and a significant loss of cardiac myocytes (Dzau et al., 2006; Jourdan-Lesaux et al., 2010). The post-MI heart undergoes a complex multiphase healing process, involving 3 overlapping phases: the inflammatory, proliferative and maturation phases (Fraccarollo et al., 2012; Frangogiannis, 2006, 2008, 2012; Pfeffer and Braunwald, 1990) (**Figure 1**). In the inflammatory phase, apoptotic and necrotic cardiomyocytes release cytokines that signal for the recruitment of neutrophils and monocytes (Fraccarollo et al. 2012). Upon arrival of these immune cells to the ischemic tissue, there is a cascade of neurohormonal and intracellular signalling events that further mobilizes and activates more immune cells, namely neutrophils and macrophages, to remove debris from the infarct area (Fraccarollo et al., 2012; Frangogiannis, 2008; Sutton and Sharpe, 2015). After the removal of cellular debris, macrophages release growth factors and cytokines such as VEGF and TGF-β leading to the maturation of granulation tissue through angiogenesis and the promotion of fibroblast proliferation, marking the beginning of the transition from the inflammatory phase to the proliferation phase (Fraccarollo et al., 2012; Nahrendorf and Swirski, 2013; Pfeffer and Braunwald, 1990). During the proliferative phase, fibroblasts migrate into the

infarct where they respond to TGF-β1, fibronectin extra domain A and mechanical tension causing them in to undergo a phenotypic change to myofibroblasts (van den Borne et al., 2010; Dobaczewski et al., 2011; Fraccarollo et al., 2012; Sutton and Sharpe, 2015). During the maturation phase, these "new" myofibroblasts, which have smooth muscle-like qualities including the ability to contract, secrete large amounts of extracellular matrix (ECM) proteins, primarily collagen, into the infarct. The deposition of ECM forms the collagenous scar which serves as mechanical support to protect the heart from ventricular rupture and is termed reparative fibrosis (Fraccarollo et al., 2012; Sutton and Sharpe, 2015). Although this scar is necessary to prevent rupture, maturation of the scar introduces its own pathophysiologic complications. Initially there is apoptosis of fibroblasts and vascular cells (Frangogiannis, 2008). The rigid scar, which does not contribute to the synchronous beating of the heart, leads to cardiac dilation, cardiac hypertrophy and in some cases cardiac failure (Dzau et al., 2006; Fraccarollo et al., 2012; Jourdan-Lesaux et al., 2010; Kempf et al., 2012; Pfeffer and Braunwald, 1990). Since this thesis focuses on the role of the macrophage, more background information on this cell type is provided in the following section.

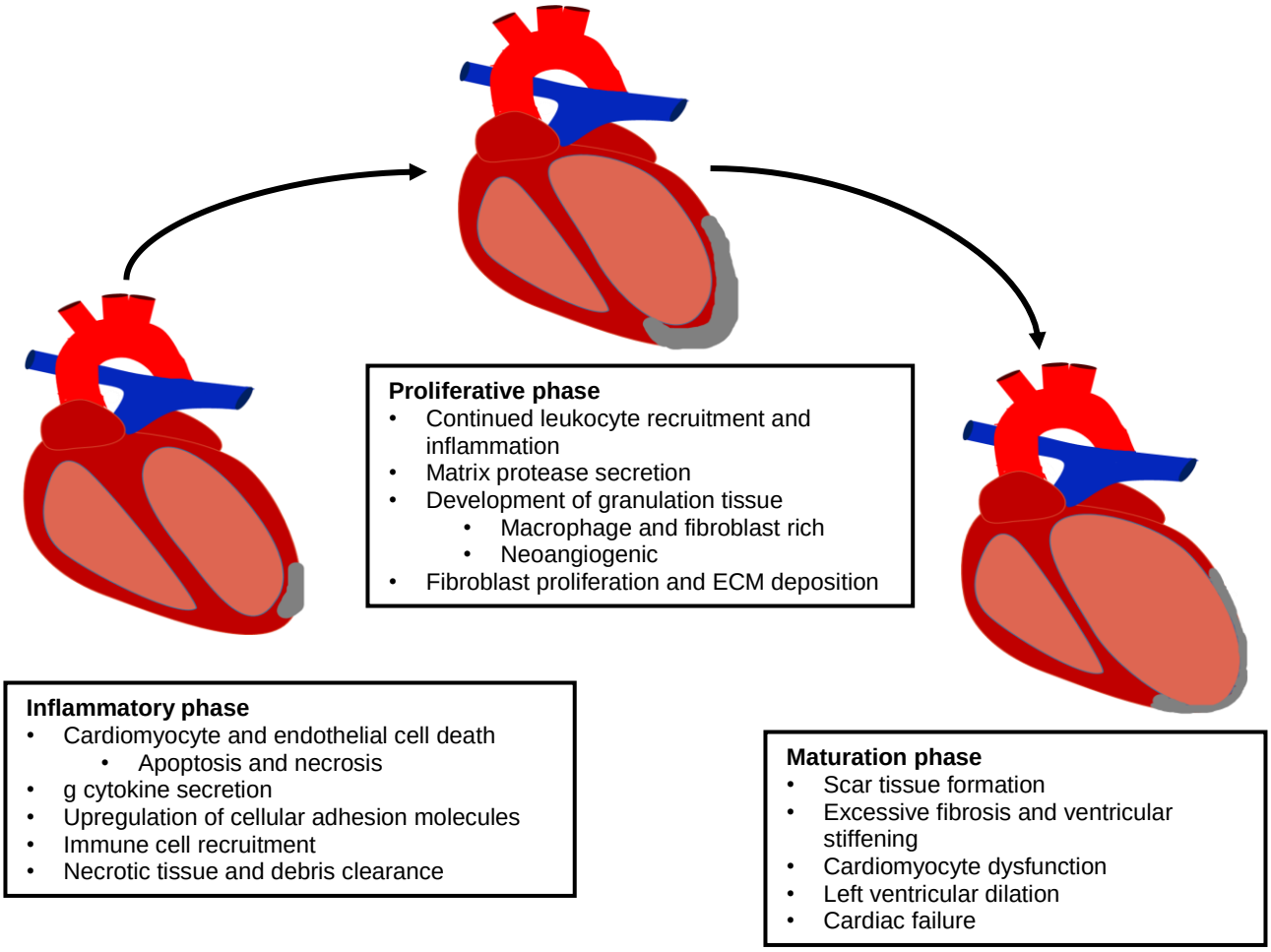

Figure 1. **Evolution of the infarcted myocardium**. MI results in the activation of a multiphase healing process, involving 3 overlapping phases: the inflammatory, proliferation and maturation phases. This repair process prevents ventricular rupture, but it is insufficient to protect the myocardium from massive tissue loss and adverse remodeling.

1.3 Macrophages

Immune cells are primarily responsible for maintenance of healthy tissue, and repairing sick or damaged tissue. Derived from myeloid or lymphoid origins, there are several different immune cells from lymphoid natural killer cells to phagocytic tissue macrophages (Baltimore et al., 2008). Macrophages are of the most abundant immune cells in the body. All macrophages, regardless of their resident location, participate in the detection of pathogens and damaged tissue, as well as the clearance of cellular debris (Pinto et al., 2014b). This occurs through macropinocytosis, a process involving a variety of pattern recognition receptors such as toll-like receptor-4 (TLR-4) mediated identification of antigens, and the secretion of chemical factors (Lim and Gleeson, 2011). It is important to note that macrophages can be classified into two broad categories: M1 and M2 phenotype macrophages; although this is a simplification and there are subsets within each category (Frangogiannis, 2012; Gordon, 2003; Mantovani et al., 2004). M1 macrophages are considered to be pro-inflammatory and mediate the initial stages of inflammation after injury/insult; while M2 macrophages have an opposing function, as they are anti-inflammatory, and promote wound healing and regenerative processes such as angiogenesis to help return the tissue to its natural state (Frantz and Nahrendorf, 2014; Gordon, 2003; Mantovani et al., 2004; Nahrendorf et al., 2007, 2010; Zhang and Wang, 2014). Differences in these cells are also apparent in expression of cell surface molecules. For example, expression of Ly-6C on the surface is method of identification. Classical, M1 macrophages are characterized by high Ly-6C on the surface with predominant expression of TNF-α and IL-1β, while alternative M2 macrophages, display low Ly-6C on the surface with expression of IL-10 and Arginase-1 (Nahrendorf and Swirski, 2013).

The heart has its own resident macrophages known as cardiac tissue macrophages (cTMs). The cTMs differ from many other macrophages as they display an alternatively active, M2-like phenotype (Pinto et al., 2012). cTMs interact with other cardiac cell types and play an important role in cardiac homeostasis. It has been shown that cTMs are involved in capillarization of the myocardium, which may be achieved through neuropilin1 (NRP1) signaling and direct interaction with endothelial tip cells to promote anastomosis (Fantin et al., 2010). cTMs also play a role in controlling age-dependent fibrosis, particularly at the epicardial level (Biernacka and Frangogiannis, 2011; Pinto et al., 2014a). Maintenance of the epicardium is critical, as it contains multi-potent progenitor cells that have the ability to differentiate into endothelial cells, fibroblasts, and smooth muscle cells in the event of cardiac injury (Chong et al., 2011; Smart et al., 2007).

Evidence continues to accumulate demonstrating the importance of resident macrophages in maintaining the optimal cardiac environment. Understanding how macrophage dysfunction can lead to a variety of pathophysiological conditions is likely to improve therapies for treating the diseased heart.

1.3.1 Macrophage Response to Myocardial Infarction

Macrophages play a vital role in the healing of cardiac tissue after infarction. It is important to remember that macrophages are a plastic cell with 2 main phenotypes (M1 and M2) that are derived from the differentiation of monocytes (Gordon, 2003; Mantovani et al., 2004; Zhang and Wang, 2014). The inflammatory response after MI is

initiated by the release of cytokines from injured/dying cardiomyocytes, which stimulates the recruitment of neutrophils and monocytes (Sutton and Sharpe, 2015). Neutrophils and monocytes are among the first cell populations recruited to the infarct area post-MI, arriving within an hour and persisting in the myocardium for several days (Jung et al., 2013). The sustained inflammatory environment in acute MI causes the release of macrophage colony-stimulating factor (M-CSF) leading to the phenotypic transition of monocyte to macrophage (Frangogiannis et al., 2003). The polarization state of the macrophage (M1 vs. M2) depends on additional stimuli received from the cell's environment and determines the mode of action of that particular cell (Mantovani et al., 2004). M1 macrophages are known to be pro-inflammatory and are found in cardiac tissue soon after MI. This pro-inflammatory phase is necessary to promote the removal of debris and to initiate healing from other immune cells. M2 macrophages on the other hand, oppose the action of the M1 as they are anti-inflammatory and pro-wound healing (Nahrendorf et al., 2007, 2010; Zhang and Wang, 2014). M2 macrophages are found in significant numbers later in the infarct healing process, at approximately 7 days post-MI. M2 macrophages are associated with infarct healing, and a shift towards an increased M2:M1 ratio is beneficial for the resolution of the inflammatory state and enhancement of angiogenesis and decreased scar size (Harel-Adar et al., 2011). It is important to note that although the macrophage response is necessary acutely, prolonged activation of macrophages results in excessive scarring, cardiac stiffening and heart failure (Fraccarollo et al., 2012). In addition to cTM's, there are sources for recruited macrophages. The injured myocardium releases cytokines such as stromal cell-derived factor 1 (SDF-1) and vascular cell adhesion molecule (VCAM) to mobilizes additional

monocytes/macrophages from two other primary resources. In the bone marrow, hematopoietic stem cells are signalled through specific adhesion molecules such as ITGA α4β1 and CXCR4, to initiate the production of mononuclear cell types needed for repair (Lo Celso and Scadden, 2011; Ehninger and Trumpp, 2011), and monocytes are stimulated to be released and home to the infarct area where they differentiate into macrophages upon arrival (Dewald, 2005). There also exists a reservoir of monocytes within the spleen, which are mobilized post-MI and contribute significantly to the macrophage population found during the MI healing process (Swirski et al., 2009). Biomaterial therapy may be an attractive strategy to regulate macrophage function in the infarcted myocardium for promoting improved repair/regeneration while not causing excessive activation and further damage.

1.4 Rationale for Biomaterials

1.4.1 Current Treatment of MI

The primary goal in treating acute MI is to restore blood flow to minimize the size of the infarct and decrease the amount of cellular trauma to cardiac tissue. Current medical practice generally consists of a combination of surgical or pharmacological techniques (Steg et al., 2012; Wijns et al., 2010). Primary surgical techniques utilized to reperfuse the system are the implantation of stents and coronary artery bypass surgery (Wijns et al., 2010). A variety of pharmacological agents are also used either to avoid or complement surgical techniques. Thrombolytics are an option to circumvent potentially invasive surgical methods as they are designed to break up clots in order to restore blood flow (Antman et al., 2004). Other therapies include the use of vasodilators and blood

thinners in order to promote blood flow and reduce the risk of further clot formation (Antman et al., 2004; Steg et al., 2012; Wijns et al., 2010). All these therapeutic techniques aim to restore cardiac perfusion; while further medication is prescribed in order to manage patient symptoms and prevent further damage to the structural components of the heart. Despite the success of these treatments in saving and improving the quality of life of patients, they do not address the underlying cause of the disease and more importantly, do not replace the tissue that is lost. Since the heart has a very low capacity for regeneration, new treatments are required in order to grow new tissue and heal the heart at the cellular and molecular level.

1.4.2 Potential of Biomaterials in MI Therapy

Over the last decade there are has been considerable research dedicated to the development of biomaterials, both synthetic and natural, to aid in the healing process post-MI (Ahmadi et al., 2014; Jourdan-Lesaux et al., 2010; Kuraitis et al., 2012; Rane and Christman, 2011; Suuronen et al., 2006, 2009). Biomaterials can take many forms from injectable hydrogels to solid patches and can serve a variety of purposes. A left ventricular restraint is a device that is surgically implanted on the outer wall of the heart in order to provide increased mechanical support to the weakened ventricle of the infarcted heart (Rane and Christman, 2011). Cardiac patches, which can be created in the lab and sutured or applied to the surface of the tissue at the site of myocardial injury, have also been employed. These integrate with the host tissue and can be used to deliver therapeutics such as drugs, growth factors or small molecules (Rane and Christman, 2011). Recently, there has been an increasing amount of research into injectable

hydrogels that can be delivered directly into the cardiac tissue. Injectable biomaterials are advantageous as they are less invasive than cardiac patches which require surgical procedure. However, injection must be precise as biomaterial that leaks into the ventricle would gel causing blockage of systemic vessels. Hydrogel materials are designed to remain liquid at cold temperature but gel at physiological temperatures upon injection. Although much research has been performed in the development of biomaterials to enhance cell transplantation therapies, it is increasingly evident that biomaterials can also be effective on their own, independent of cells. Thus far, various biomaterials have been shown to improve left ventricular ejection fraction (LVEF), reduce infarct size and scarring, and enhance tissue viability, angiogenesis, and cardiomyogenesis. It is clear that biomaterials are capable of improving cardiac repair at a cellular level rather than just controlling the effects of deteriorating function (Jalil and Seliktar, 2015; Pascual-Gil et al., 2015; Venugopal et al., 2012; Wang and Christman, 2015).

Post-MI, the composition of the cardiac ECM undergoes considerable change as it is remodeled through the inflammatory, proliferative and maturation phases of ischemic injury (Li et al., 2014). Since a cells function is controlled, in part, by interactions with the ECM environment, the cardiac ECM changes that occur post-MI can significantly affect the reparative response of the cells in the heart (Bayomy et al., 2012; Dobaczewski et al., 2011; Fan et al., 2014) (**Table 1**). The use of biomaterials may be a promising therapy to circumvent adverse compensatory events initiated by ECM changes post-MI.

	Cardiomyocytes	Macrophages	Fibroblasts	Endothelial Cells
Cellular Dysfunction	- Cell death - Minimal regeneration	- M1 invasion - Inflammation	- Myofibroblast phenotype - Extended activity	- Apoptosis and necrosis - ROS production
Adverse Function	- ↓Contractility - Ventricular thinning	- Excessive MMP activity - Pro-nectrotic signaling	- ECM deposition - Cardiac hypertrophy - Stiffening	- ↓ Cardiac perfusion - Sustained hypoxia

Table 1. **Cell responses and functional changes post-MI**. The response of different cell types after MI and the resultant negative outcome of these responses that may contribute to heart failure development.

1.4.3 Use of Collagen Matrices in Cardiac Regeneration

Collagen, the most abundant ECM protein in the heart, is widely used in cardiac tissue engineering applications. The ECM is responsible for providing structural support to the heart as an organ by forming networks for cellular adhesion and communication (Fan et al., 2014). Surface adhesion molecules on the cell's surface such as integrins (ITGs) and immunoglobulins bind to the ECM initiating internal signalling cascades altering cellular activity (Tallawi et al., 2015). Type 1 collagen-based biomaterials delivered as patches or injectable hydrogels have demonstrated the ability to reduce scar size, adverse remodeling and to improve function of the MI heart (Ahmadi et al., 2014; Blackburn et al., 2015; Serpooshan et al., 2013; Xu et al., 2014). The injection of a biomaterial also creates the opportunity for localized cell treatment to an injury. Small intestinal submucosal ECM (SIS-ECM), which is composed primarily of various

collagens (type 1 most abundantly), was injected with and without circulating angiogenic cells (CACs) into a mouse model of MI (Toeg et al., 2013). Both treatments lead to greater LV posterior wall thickness and reduced infarct size with newly formed cardiomyocytes and/or cardiac progenitor cells were observed. In other work, cardiac ECM, derived from the decellularization of porcine myocardium, has been shown to attenuate adverse remodeling and the deterioration of cardiac function of the MI heart in both rats and pigs (Seif-Naraghi et al., 2013; Singelyn et al., 2012). In pigs, there was visible muscle retention in the endocardium of cardiac ECM-treated animals with neovascularization observed below these beds of cardiomyocytes (Seif-Naraghi et al., 2013). The above examples highlight the use of in vivo derived ECM biomaterials in the treatment of MI. Chemically crosslinked collagen hydrogels are also effective at improving function post-MI. Previous work out of the Suuronen lab has demonstrated that the injection of an EDC/NHS cross-linked collagen matrix is able to improve angiogenesis, reduce inflammation and cell death, and prevent further loss of cardiac function after MI. It has also been shown that collagen matrices are able to improve therapeutic effects of circulating angiogenic cells (Ahmadi et al., 2014; Kuraitis et al., 2011, 2012; Suuronen et al., 2006, 2009). More recently, our group identified that injection of the collagen matrix 3 hours post-MI leads to superior healing compared to injection at later time-points. There was also a more predominant M2 response at 2 days post injection and increased vascularity in the infarcted area (Blackburn et al., 2015). This work demonstrates the viability of the collagen matrix therapy in treating the MI heart; however the exact mechanisms of action are still unclear.

1.4.4 Macrophage Response to Biomaterial Therapy

Macrophages are highly plastic cells that are very sensitive to their surroundings. Therefore, biomaterials have the potential to vastly alter macrophage function and remodelling in the post-MI heart. Composition of the biomaterial is important; the culture of monocytes on polyethylene terephthalate yields an increased M1:M2 response compared to culture on polypropylene, which had the opposite effect: greater M2 polarization (Grotenhuis et al., 2013). This illustrates that macrophages are responsive to biomaterial therapy and can be differentially polarized. Other work has aimed to identify polarization, as well as subsequent localization, of different cell colonies in response to a variety of different biomaterial patches. Specifically, in one study, biomaterials that predominantly stimulated M1 polarization, clusters of M1 macrophages were observed around the border of the material, while the few M2 macrophages that were present had infiltrated the material's centre and contributed to constructive remodelling (Brown et al., 2012). Physical characteristics of the biomaterial such as fiber diameter and material stiffness have also been studied. Notably, for M0 macrophages cultured on electrospun polydioxanone (PDO), greater expression of the M2 marker arginase and reduced expression of the M1 marker iNOS was observed on scaffolds with larger fibers and pore sizes, suggesting that larger fiber and pore size promote the differentiation of M2 macrophages (Garg et al., 2013). Similar findings were reported by a group using electrospun poly(ε-caprolacetone) (PCL) as the biomaterial suggesting physical characteristics may be equally as important as chemical composition (Wang et al., 2014). Macrophage phenotype and function plays a significant role in the remodeling of the

post-MI heart, therefore how a biomaterial affects macrophages may ultimately decide the overall success of a biomaterial therapy.

1.4.5 Importance of Macrophage Migration in Biomaterial Therapy

An advantage of biomaterial therapy is that it provides immediate structural support to injured cells following MI. One important aspect of this type of therapy is the ability of immune cells to migrate through the matrix in order for its therapeutic effects to be exerted both within the material and in its periphery. Macrophage migration can be chemokine directed and mediated through matrix metalloproteinases (MMP). Not only do macrophages have the ability to migrate, they have a diverse chemokine secretion profile that is capable of activating migratory pathways in a paracrine fashion. For example, myoblast migration was greatest in conditioned media from M2 polarized macrophages compared to M1 (Brown et al., 2012). Therefore, in biomaterials, there is the potential to control macrophage phenotype and their ability to promote the recruitment of different cell types required for the regeneration of cardiac tissues.

1.5 MicroRNA Generation and Processing

Emerging in science are a class of small non-coding RNA termed microRNA (miRNA or miR). Generally, only 22-25 nucleotides in length, miRNAs regulate gene expression through binding of the 3'UTR and negatively regulating translation of the target genes mRNA (Ambros, 2004; Bartel, 2009; Dorn, 2011; Port et al., 2011; Rayner et al., 2010; Small et al., 2010). Although the majority of miRNA is encoded within intergenic strands, there is also portion of miRNA that is encoded by intronic DNA.

Intronic miRNAs are spliced out with a spliceosome where it goes for further processing in the cytoplasm. Intergenic miRNAs are spliced away from the DNA with the protein duplex Drosha-DGCR8, which is then exported the cytoplasm where Dicer prepares the mature miRNA for binding to the RNA-induced silencing complex (RISC). At this point, the miRNA can be packaged it microvessicles such as exosomes for release or may bind to the 3'UTR of the mRNA strand where it causes repression of translation or mRNA degradation (Bartel, 2004; Dorn, 2011). Due to the complex nature of miRNAs with biogenesis originating from intergenic DNA and intronic processing, they exhibit control over many biological processes with high fidelity. Adding to this is the ability for miRNAs to target several genes governing the same biologic process. For example, miR-92a targets several genes associated with ECM interactions, increasing the chance that it will produce the desired outcome (Bonauer et al., 2009; Nouraee and Mowla, 2015).

1.5.1 MicroRNA in Cardiovascular Disease and MI

Growing evidence suggests that miRNAs play a large role in a wide range of cardiovascular diseases from chronic genetic illnesses to acute onset syndromes. miRNA profiling of cardiac tissue identified approximately 200 miRNAs which were constitutively expressed and regulated in diseases such as cardiac hypertrophy and heart failure (Dorn, 2011). Animals in a heart failure model showed recovering miRNA profiles after mice received left ventricular assist devices demonstrating in importance of miRNA and subsequently mRNA on progression and mediation of heart failure (Dorn, 2011). During MI, several changes that occur at the molecular level contribute to the end fate of the cardiac tissue. One of these molecular factors is alterations in expression

miRNAs. It has been shown that after MI, several miRNAs have altered expression in cardiac tissue, which contribute to disease pathology and/or wound healing (Bonauer et al., 2009; Dong et al., 2009; Hu et al., 2011; Kukreja et al., 2011; Port et al., 2011). For example, miR-21 targets genes such as Spry1 and PTEN in fibroblasts which contribute to cardiac fibrosis post-MI (Dong et al., 2014; Gong et al., 2014). miR-92a is also significantly up-regulated post-MI, which has very negative implications as this is associated with anti-angiogenic and pro-inflammatory functions (Bonauer et al., 2009; Kukreja et al., 2011). Currently, there have been few studies which characterize the effect of biomaterials on miRNA expression during acute cardiac events. As we were interested in investigating which microRNAs may be playing a role in the matrix-induced post-MI healing, we performed microarray analysis on 2d infarct tissue after injection with matrix at 3h post-MI. Matrix treatment resulted in significant alterations in the expression of detrimental miRNA, miR-92a (Chiarella-Redfern 2015). With technology advancing and becoming more accurate for molecular monitoring, it soon may be possible to use miRNAs as biomarkers or as therapeutic targets for cardiac conditions to facilitate early diagnosis and treatment. However, given the vast and complex nature of miRNA expression, further research must be done to better understand the roles and mechanistic action of miRNAs in cardiovascular disease.

1.5.2 miR-92a Regulation and Functions

Located at position 31 on the long arm of chromosome 13 is a cluster of microRNA known as the miR-17-92 cluster. This group of miRNAs stretches along a distance of 800bp on the third intron of the *cl31orf25* gene (Hayashita et al., 2005; Ota et

al., 2004). The miR-17-92 cluster has been shown to play a part of many diseases; of particular interest is miR-92a, which has been shown to participate in the pathophysiology of lung cancer, hepatocellular carcinoma, breast cancer, and ventricular remodelling post-MI to name a few (Hinkel et al., 2013; Lin et al., 2013; Nilsson et al., 2012; Shigoka et al., 2010; Zhang et al., 2014). Mechanistically, miR-92a has been shown to target ITGAα5 and αV, SIRT1 and S1Pr1 that ultimately affects angiogenesis, inflammation, and migration. In a breakthrough study by Bonauer et al in 2009, it was found that forced over expression of miR-92a inhibits the formation of vascular networks, blocks sprout formation, and reduces cellular adhesion and migration. Subsequent anti-miR treatment resulted in increased vessel formation and improved overall cardiac function (Bonauer et al., 2009). The improvements in angiogenesis were attributed to the upregulation of ITGα5, a known target of miR-92a. Similar results were observed when pigs were treated with a locked nucleic acid (LNA)-92a after MI. Treatment with (LNA)-92a led to improved vasculogenesis, reduced scarring, and improved cardiac function (Hinkel et al., 2013). In a model of vascular injury, inhibition of miR-92a resulted in reduced inflammation as shown by decreased lesion formation (Daniel et al., 2014). MiR-92a may play a role in inflammation through known targets sirtuin-1 (SIRT1) and S1P1 receptor (S1Pr1), which directly inhibit inflammation in macrophages (Bonauer et al., 2009; Hughes et al., 2008; Yoshizaki et al., 2010). Dysregulation of miR-92a in some cancers has been associated increased invasiveness providing support for miR-92a's role in migration. In lung cancer, STAT3, an upstream regulator of miR-92a, increases miR-92a levels, which directly targets RECK to increase invasiveness (Lin et al., 2013). In a different study of breast cancer, the downregulation

of miR-92a improved macrophage localization and migration into tumors (Nilsson et al., 2012).

It is clear that miR-92a takes part in many biological processes. MiR-92a is known to be upregulated post-MI and is a potent inhibitor of anti-inflammatory pathways and angiogenesis, both necessary for the repair of MI. Controlling the expression and dysregulation of miR-92a offers novel therapeutic opportunities and may be a viable approach to improving myocardial repair post-MI.

1.6 Research Plan

1.6.1 Rationale

Inflammation, cardiomyocyte death, adverse cardiac remodelling, and subsequent deterioration of cardiac function are all hallmark consequences of MI. Evidence has shown that treatment of the infarcted myocardium with biomaterials post-MI is capable of reducing adverse ventricular remodelling and improving revascularization and cardiac function (Jalil and Seliktar, 2015; Pascual-Gil et al., 2015; Venugopal et al., 2012). Of particular interest is a chemically crosslinked type 1 collagen biomaterial which improves overall cardiac function attributed to reduced infarct size, inflammation and cell death, enhanced angiogenesis, and an altered macrophage polarization profile (Ahmadi et al., 2014; Blackburn et al., 2015). The biomaterial's ability to influence macrophage function post-MI is key in limiting the chronic inflammation and overall cell death. Although promising, an exact mechanism of action has not been defined. With the high activity of miRNA in cardiovascular disease, it is believed they play a key role in the adverse of

implications of MI. In previous miRNA profile studies from the lab (unpublished), it was shown that injection of the collagen biomaterial at 3h post-MI resulted in significantly decreased expression of the anti-angiogenic, pro-inflammatory miR-92a at 2-days post-treatment. It is believed that the efficacy of the biomaterial in treating the MI heart may be, in part, due to its ability to regulate miR-92a expression. Since less inflammation was observed in the post-MI heart, and given that miR-92a has targets that regulate inflammation, this study examined the ability of the matrix to control macrophage function through a miR-92a mechanism.

1.6.2 Aims and Objectives

1. To determine if collagen matrices are able to regulate macrophage phenotype and function through regulation of miR-92a.
2. To identify mechanisms by which miR-92a can control the functionality of different macrophage phenotypes.

1.6.3 Hypotheses

We hypothesize that a collagen matrix will promote an anti-inflammatory/pro-wound healing macrophage phenotype through the downregulation of miR-92a expression. Subsequently, we believe that reduced miR-92a levels will result in superior migration of wound healing macrophages.

Materials and Methods

2. Materials and Methods

All animal work was performed with the approval of the Animal Care Committee at the University of Ottawa Heart Institute

2.1 *In Vivo* and *In Vitro* Sample Collection

2.1.1 Animal Model of MI and Surgical Technique

One week prior to surgical procedure, 7-9 week old female C57BL/6J mice (Charles River, Sherbrooke, QC, Canada) arrived at the Heart Institute to acclimate. To avoid unnecessary pain/distress, 1 hour prior to surgery animals were injected 0.1mL buprenorphine. Mice were anesthetized with gaseous isoflurane with 2% oxygen and underwent irreversible ligation of the left anterior descending coronary artery (LAD) in order to induce MI as described in Ahmadi et al. 2014. In preparation, mice were intubated with a 20G catheter (BD Bioscience) and cleared of hair from the chest with hair removal cream. Mice were then transferred to a heated operating platform where an incision was made between the 4^{th} and 5^{th} rib which were then spread to reveal the heart. The LAD was ligated using a 6.0 silk suture (Syneture) with two stitches to produce appropriate blanching. The rib separator was removed and skin was closed with #5 synthetic thread (Syneture). Three hours post-MI mice were randomly selected to their treatment group of: i) no injection, ii) PBS injection or iii) collagen matrix injection. Animals received injections (PBS or matrix) in 3-4 intramuscular locations, 50uL total, in the infarct/peri-infarct region guided through echocardiography with a 27 ½ G syringe. Mice were sacrificed at 4h, 1d, 3d, and 7d post- injection. Cardiac tissue samples were dissected from the infarct/peri-infarct zone, non-infarcted left ventricle, and right ventricular muscle and stored in 4% PFA at -80^{o}C. RNA was later extracted for RT-qPCR for microRNA expression and target gene expression profiling.

Animals in the SHAM category underwent all the same pre-op procedures and had their chest cavities opened similar to experimental group mice, however, no LAD ligation was done.

2.1.2 BMDM Isolation and *In Vitro* Culture

Female C57BL/6J wild type mice aged 6-10 weeks were euthanized by CO_2 inhalation and cervical dislocation. Mice were then thoroughly sprayed with 70% ethanol to kill bacteria within the fur before skinning the lower half of the mice. Leg amputation occurred above the hip joint as to not expose the inner marrow to the external environment while being transferred in a sterile tube containing PBS. Small scissors were used to clean muscle away from the femur. One cut was made immediately superior to the knee and inferior to the hip to create an open-ended tube to flush bone marrow. Using a 25G needle attached to a media filled syringe, the needle tip was inserted into one end of the bone and marrow was flushed into a clean 50mL Falcon tube. The media used consisted of DMEM high glucose (Gibco), 20% L929 conditioned media, 10% FBS (Gibco) with pen/strep added. The cell-media mixture was then mixed through pipetting to break up larger chunks of marrow and divided equally into (n-1; n= # of legs) 150mm diameter plates. For example, if 3 mice were sacrificed, 6 legs were harvested and media containing cells were divided into 5 plates. Plates were then topped up with media to a total volume of 25mL and placed at 37^{o}C for 4 days. At day 4, more media was added to provide nutrition to the cells. If too few cells were stuck down by day 4, cultures were spiked with 3-5mL of pure L929 conditioned media to enhance macrophage differentiation. Media was changed at day 6 if cells were confluent, or left till day 7 until

ready for experimental use, typically day 7. Cells were lifted using 6mL of 5mM EDTA/HBSS (without Ca^{2+}/ Mg^{2+}) followed by refrigeration at 4ºC for 13 minutes. Plates were then gently scraped and cells were collected into a 50mL Falcon tube containing 2-3mL media. Prior to centrifugation, 10µl of media was removed and added to a counting slide (BioRad) for counting by the TC10 Automated Cell Counter (BioRad), while remaining cells were spun at 1300rpm for 5 min to pellet cells for EDTA/HBSS removal and resuspension.

For experiments comparing matrix vs. tissue culture polystyrene (TCPS control), cells were plated on matrix at a density of 4.0 $x10^6$ cells, while cells seeded on TCPS were plated with a density of $2.0x10^6$ cells. Cells were seeded at different densities to accommodate for loss of cells during collagenase breakdown of matrix. All experiments requiring transfection with miR-mimics or anti-miRs were seeded with $2.0x10^6$ cells.

2.2 Treatment Conditions

2.2.1 Matrix Preparation

The collagen matrix was synthesized in a 5ml Eppendorf bullet tube chilled on ice as previously described in Blackburn et al 2015. Collagen was crosslinked using 1ml of 4.36 mg/ml type 1 rat tail collagen (Corning, Corning NY) and 200µL of crosslinking solution. The crosslinker consisted of 0.1M 2(-N-morpholino) ethanesulfonic acid (MES) buffer (pH~6.0) added to 2.5mg 1-Ethyl-3-(3-dimethylaminopropyl)carbodiimide (EDC) and 1.5 mg N-hydroxysuccinimide (NHS) forming a 1:1 molar ratio. After thorough mixing of crosslinker and collagen, 400µL of PBS was added followed by 100µL of 40%

chondroitin sulfate-C (Wako, Osaka, Japan) in Mg^{2+}/Ca^{2+} free PBS. There was thorough mixing after the addition of each ingredient to ensure homogenous mixture. Using 1N NaOH, the collagen solution was adjusted to a pH of 7.2 ± 0.2 per colorimetric pH paper. For *in vivo* injections, 200µL of collagen was added to 1cc syringes with a 27 ½ G needle (BD Bioscience) and placed on ice to avoid gelation while mice were prepared and mapped using echocardiographs. During *in vitro* experiments 225µL of matrix was evenly spread across the surface of 6-well plates and placed at 37ºC for 20 minutes for gelation. After gelation, the matrix was washed with PBS for 45 minutes twice and left to sit overnight in PBS at 37ºC. Gels were made on the day of injection for *in vivo* experiments or 1 day prior to use for *in vitro* experiments.

2.2.2 Transfection of BMDMs with anti/mimic microRNAs

miR-92a inhibitors and mimics (Dharmacon) were reconstituted to a final concentration of 20µM with ultrapure RNase free water (Invitrogen). The process for antimiR and miR-mimic transfection are the exact same. The transfection mixture was made by mixing 5µL of mimic with 200µL OptiMEM (Gibco), which was mixed by pipetting. This reaction was scaled up based on the number of individual wells needed to transfect. Once the transfection mixture was added to the wells, 2µL of lipofectamine RNA iMAX were added directly to the wells and swirled to mix. After incubation at room temperature for 30 minutes, cells suspended in antibiotic free media (DMEM high + 10% FBS) were seeded at a density of $2.0x10^6$ cells. After the addition of cells, plates were placed at 37ºC for 48 hours. All miR-92a inhibitor and mimic transfection experiments were run against a control antimiR or control miR-mimic, respectively.

2.2.3 Macrophage Phenotype Polarization

The current cell culture protocol is sufficient to generate large amounts of M0 macrophages, however, to determine the role of macrophage phenotype on function, macrophages need further help to polarize. On day 6, cells were lifted, counted and resuspended in a volume that allows for 2mL of media to be added to individual wells of a 6-well plate. To induce the M1 phenotype, 2μL [1μg/mL] of lipopolysaccharide (LPS; 1mg/mL; Sigma) and 2μL [100ng/mL] of interferon gamma (IFN-γ; 100ug/ml; R&D Systems) were added to each well to be polarized. The M2 phenotype was induced by adding 2μL [10ng/mL] of IL-4 (100μg/ml; R&D Systems) to each well. Cells were then placed at 37^{o}C to incubate for 24 hours before being lifted for further treatment on matrix or TCPS.

2.3 RNA isolation

2.3.1 Cardiac Tissue RNA Isolation

The lab bench was thoroughly cleaned with RNase Away (Thermo Scientific) to avoid any sample being compromised by RNase contamination. One scoop of 2.0mm zirconium silicate beads (Ideal Scientific) was placed in a clean 1.5mL Eppendorf tube followed by 1ml of TRIzol and cardiac tissue. The tissue was then homogenized at 4^{o}C in a bullet blender (Integrated Science Solutions) for 4× 5 minute intervals at an intensity of 9. The supernatant was then collected and transferred to a clean 1.5mL Eppendorf tube with 200μL of chloroform added to the homogenate. The sample was mixed by intense shaking for approximately 15 seconds and incubated at room temperature for 15 minutes.

Following separation of the TRIzol-chloroform mixture, the tubes were spun at 12000g for 15 minutes at 4ºC. The top phase containing RNA was then transferred to a clean 1.5mL tube for washing and precipitation with 1.5x the transferred volume with 100% ethanol (eg: 400µL of top phase = 600µL 100% ethanol added). The washed RNA was then moved to the miRneasy Micro Kit (Qiagen) for isolation on a column. RNA binds the filter of the column as the ethanol passes through during the first spin. Once the ethanol is removed, several wash steps occur with the Qiagen's RWT and RPE wash buffers, respectively, followed by a wash with 80% ethanol. Spin columns were then placed in a clean 1.5mL tube with 25µL of ultrapure water added to the column for the final spin. Water dissolves RNA allowing it to be released from the filter during the final spin at 15000g for 1 minute.

2.3.2 Cultured Cell RNA Isolation

The isolation of RNA from cultured cells is very similar to cardiac tissue RNA isolation except there is no bullet blending homogenization, and instead of transferring the upper layer of RNA to a spin column, it is transferred to a clean 1.5mL Eppendorf tube. In experiments where cells are on the plate directly, TRIzol was added directly to the well, pipetted up and down to wash the surfaced of the plate and transferred to the Eppendorf tube. For matrix-cultured cells, the matrix was first dissolved in 200µL of 2500units/ml type 1 collagenase (Sigma) with 1800µL 3mM $CaCl_2$/HBSS at 37ºC for 30 minutes. The now liquefied matrix was collected in a 15ml tube and spun for 6 minutes at 1300rpm. The supernatant was aspirated off and 1mL of TRIzol was added directly to the cell pellet before transferring to a 1.5mL Eppendorf tube. Chloroform was then added,

shaken to mix, and allowed to separate for 15 minutes at room temperature before centrifuging at 12000g for 15 minutes. The clear, top phase was removed and transferred to a clean 1.5mL tube where 500μL isopropanol was added. The samples with isopropanol were mixed by inversion and allowed to incubate at room temperature for 10 minutes before spinning at 12000g for 10 minutes at 4^{o}C. The clear isopropanol supernatant was removed carefully as to not remove the small, white RNA pellet. The final step included washing with 1mL of 75% ethanol and centrifugation at 7500g for 5 minutes at 4^{o}C. After removal of the ethanol, the RNA pellet was allowed to air dry for 10-15 minutes, depending on the size of the pellet, before reconstituting the RNA pellet in 15-20μL of ultrapure RNase free water (Invitrogen).

2.3.3 RNA Quantity and Quality

All RNA was analyzed using the NanoDrop-1000 Spectrophotometer with V3.3 Software (Thermo Scientific). The machine was blanked with ultrapure water prior to initial sample. 1μL of sample was placed on the pedestal with the closed arm allowing the machine to display RNA concentration in ng/μL, 260/280 (measure of protein contamination), and 260/230 (measure of PCR inhibitors). All samples used had 260/280 $\geq$ 1.9 and 260/230 $\geq$ 1.5. If samples appeared "messy" with low 260/280 and low 260/230, samples were run through the wash phases of miRneasy Micro Kit (Qiagen) as previously described. This cleans the samples to ensure successful and reliable PCR data.

Due to the nature of the homogenization process, RNA isolated from cardiac tissue is susceptible to fragmentation thus requiring one further quality check with the

Agilent RNA 6000 Nano Kit (Agilent Technologies) and the 2100 Bioanalyzer instrument with the 2100 Expert Software (Agilent Technologies). This software is designed to measure RNA integrity by separated RNA based on weight. After the chip was primed with gel-die mix, RNA marker and ladder, 1μL of denatured RNA was placed into their respected wells of the chip. The chip was then mixed by vortexing at 2400rpm for 1 minute before commencement of bioanalyzer. The readout displays an RNA integrity number (RIN) which is used as a ranking system out of 10 to grade the RNA, with 10 being the best. All tissue isolated RNA was found to have a RIN $\geq$ 8.0 which is considered intact and usable for PCR.

2.4 Quantification of miR-92a and Associated Targets

2.4.1 Reverse Transcription and qPCR for miRNA Target Genes

After the search of several databases (miRDB, miRBase, Target Scan) and literature searches, targets of miR-92a were identified and primers were ordered for the study of gene expression. Along with known targets, genes associated with macrophage polarization and genes known to play a role in miR-92a regulation were also tested in cardiac tissue and BMDMs:

Common Name	Gene Abbreviation	Primer Direction	Sequence
Integrin α5	ITG α5	Forward	CTCCCTCTACAACGTCTCAGG
		Reverse	CATCTCCATTGGTATCAGTGGC
Integrin αV	ITG αV	Forward	TTGATTCAACAGGCAATCGAGA
		Reverse	AGCATACTCAACGGTCTTTGTG
Sphingosine-1-Phosphate Receptor	S1Pr1	Forward	ATGGTGTCCACTAGCATCCC
		Reverse	CAGCCGTCTCTGTGTCACAAA
Sirtuin 1	SIRT1	Forward	CAGCCGTCTCTGTGTCACAAA
		Reverse	GCACCGAGGAACTACCTGAT
Signal Transducer and Activator of Transcription 3	STAT3	Forward	CAATACCATTGACCTGCCGAT
		Reverse	GAGCGACTCAAACTGCCCT
Interleukin-10	IL-10	Forward	GCTCTTACTGACTGGCATGAG
		Reverse	CGCAGCTCTAGGAGCATGTG
Inducible Nitric Oxide Synthase	iNOS	Forward	GTTCTCAGCCCAACAATACAAGA
		Reverse	GTGGACGGGTCGATGTCAC
Housekeeping	18s	Forward	GTAACCCGTTGAACCCCATT
		Reverse	CCATCCAATCGGTAGTAGCG
Housekeeping	HPRT	Forward	TCAGTCAACGGGGGACATAAA
		Reverse	GGGGCTGTACTGCTTAACCAG

Table 2. **List of Genes and Primers used in RT-qPCR analysis.**

RNA was reverse transcribed to cDNA using IScript Reverse Transcription Supermix for RT-qPCR (Bio Rad). cDNA mixture was composed of 4μL supermix, 500ng - 1ug of RNA, and ultrapure water totalling 20μL. The sample was mixed thoroughly and pulse centrifuged to collect contents at the bottom before placing in the Mastercycler Gradient (Eppendorf). The Mastercycler RT program is as follows: 25°C

for 5min followed by 42°C for 30min and 85°C for 10min finishing with 4ºC until samples could be diluted 1:10 and stored at -20ºC.

To organize the PCR, a mastermix for each gene of interest was prepared in triplicate to accommodate loading on the plate. The triplicate volumes of each ingredient in the reaction are: 30µL of SYBR Green Supermix (BIO RAD), 1.2µL of 10uM forward and reverse primer and 21.6µL of Ultra Pure distilled water. Prior to plating the reaction, 56µL of mastermix was combined with 6µL of cDNA. Plates were loaded with 20µL in each well, sealed with adhesive plate seals (Fisher Scientific) or cap strips (VWR) and spun for 30 seconds in Mini Plate Spinner-MPS 1000 (Labnet). The plate was then placed in the Mastercycler Realplex^2 (Eppendorf) and turned completing the 30 second at 95ºC activation followed by repeating 40 cycles of denaturation for 5s at 95°C and annealing/extension for 15s at 60°C followed by a melting curve step. Relative quantification was used with gene expression normalized to housekeeping gene expression.

2.4.2 Reverse Transcription and qPCR for miRNA Expression

The primer assays for miRNA PCR were ordered from Qiagen; miR-92a (MS00005971) and housekeeping gene RNU6-2_11 (MS00033740). RNA samples were reverse transcribed using miScript II RT kit (Qiagen), in a similar fashion to the prior RT procedure. In a 0.5mL tube, 500ng of RNA was mixed with 4µL of 5x miScript HiSpec Buffer, 2µL of 10x miScript nucleics Mix, 2µL miScript Reverse Transcriptase Mix and Ultra Pure water to a total volume of 20µL. Samples were mixed and pulse centrifuged

before being placed in the Mastercycler Gradient (Eppendorf). The MiScript RT program starts with 37°C for 60min followed by 95°C for 5min and finishes with a hold step at 4ºC until ice or freezing. The samples were diluted 1 in 8 with water and stored at -20°C until eventual use.

For the miScript PCR, one master mix per miRNA and housekeeping control to be tested was made. The triplicate volumes of ingredients are as follows: 30µL of 2x QuantiTect SYBR green PCR Master Mix, 6µL of miScript Primer Assay, 6µL of 10x miScript Universal Primer and 12µL of Ultra Pure distilled water. After mixing, 59.4µL of master mix was added to 6.6µL of cDNA in 0.5ml tube. The samples were plated in triplicate with 20µL per well, sealed with caps (VWR), spun for 30 seconds in Mini Plate Spinner-MPS 1000 (Labnet) and placed in the Lightcycler. The cycling conditions were 15min at 95°C for the initial activation step and 40 cycles of denaturation for 15s at 94°C, annealing for 30s at 55°C and extension for 30s at 70°C, followed by a melting curve step. Relative quantification of the miRNA of interest was done by normalizing to expression of the RNU6B housekeeping gene.

2.4.3 Protein Isolation and Western Blots

Transfected cells and cells plated directly on the surface of the plate were prepped for lysis by media aspiration and 2x PBS washes. Cells plated on matrix required one further step of collagenase treatment, as previously described, to release cells from the matrix. Cells were lysed directly with 2x Laemmli buffer (4% SDS, 20% glycerol, 10% 2-mercaptoethanol, 0.004% bromphenol blue and 0.125 M Tris HCl, pH approx. 6.8)

either on the plate or in a spun 15ml tube from collagen matrix treated cells. Lysis occurred for 20-30 minutes on ice before being transferred to a 0.5ml Eppendorf tube and stored at -20^{o}C.

The main running gel was made by mixing 8.0ml of water, 3.0ml of 40% acrylamide, 3.8ml of 1.5M Tris buffer (pH 8.8), 0.15ml of 10% sodium dodecyl sulfate (SDS), 0.15ml of ammonium persulfate (APS) and 0.012ml of tetramethyethylenediamine (TEMED) in a 50mL Falcon tube. The gel solution was then transferred to a gel plate where it was filled to approximately 1cm from the top. Isopropanol was added to clear any bubbles and keep the gel flat while it solidified for 20 minutes. Isopropanol was removed prior to addition of the stacking gel (7.5ml of water, 1.0ml of 40% acrylamide, 1.25ml of 1.0M Tris buffer (pH 6.8), 0.1ml of 10% SDS, 0.1ml of APS, and 0.010ml of TEMED) which was left to solidify for 30 minutes with a 10-well comb present. Samples were prepared for electrophoresis by boiling at 95^{o}C for 10 minutes then loaded, 48µL, into a 10 well 1.5mm thick, 8% sodium dodecyl sulfate-polyacrylamide gel electrophoresis (SDS-PAGE) with 8µL of Precision Plus Protein Ladder (Bio Rad). Once the gel was loaded, the running chamber was topped up with electrophoresis buffer (25mM Tris base, 192mM glycine and 3.5mM SDS with double distilled water) and electrophoresis began at 90V while the samples were in the stacking gel, then turned up to 110V for approximately 90 minutes. Once the dye-front reached the bottom of the gel, the electricity was turned off, and the gel was then transferred to a methanol activated PVDF membrane for 2 hours at 80V at 4^{o}C. The transfer buffer contained 100ml of 10x transfer buffer (25mM Tris Base and 192mM Glycine), 200ml of

MeOH and 700ml of ddH_20. Immediately following the transfer, membranes were cut and blocked in 5% milk in TBST (100ml 10x TBS (50mM Tris Base and 150mM NaCl with water, pH 7.4), 900ml ddH2O and 1ml Tween-20 (BioRad)) for 1 hour at room temperature on a rocker (Immunetics). Initial probe of blots with primary antibodies diluted in PBS + 0.1% azide, ITGAα5 (1:500; Santa Cruz; SC10729), ITGAαV (1:1000; Cell Signalling; 4711P), SIRT1 (1:1000; Novus Bio; NBP1-51641SS), S1Pr1 (1:1000; CusaBio; CSB-PA020650LA01HU), and loading control tubulin (1:1000; Sigma; T6074-200UL), were completed overnight at 4ºC with constant shaking. Primary antibodies were then removed and blots were washed 3x with TBST for 5 minutes before secondary antibody were added, 1:1000 dilution of IRDye700 conjugated anti-mouse IgG (Rockland) and a 1:1000 dilution of IRDye800 conjugated anti-rabbit IgG (Rockland), diluted in PBS-Casein (0.1% Casein, 0.1% SDS, PBS). After 1 hour, the secondary antibody was removed and blots were washed 3x TBST for 5 minutes before scanning on the Odyssey scanner (LI-COR) using Odyssey Version 3.0 Software. ImageJ was used to quantify pixels of protein bands and normalized to the tubulin loading control.

2.5 Macrophage Function Studies

2.5.1 Macrophage Adhesion by Phenotype

On day 6 of BMDM culture, macrophages were lifted, counted and resuspended as previously described. Cells were plated on 6-well plates at a density of $4.0x10^6$ cells in 2mL. Immediately, reagents were added to polarize macrophages to their M0, M1, and M2 phenotypes, then incubated at 37ºC for 24 hours. On the same day, matrix was prepared as described previously with a slight deviation. In this instance, before

spreading the matrix, a coverslip was placed in the centre of every well of the 6-well dish so to be completely covered when 300μL of matrix was added and evenly spread over the well. After 24 hours, media was removed and cells were DAPI stained, 1:1000 in PBS, at 37^{o}C for 30 minutes. Cells were then lifted and counted and seeded on matrix at a density of 4.0x10^{5} cells/mL in 1 mL of media at 37^{o}C. After 24 hours, coverslips were lifted and mounted face down on slides with fluorescent mounting medium (Dako). Slides were imaged under the Zeiss Axio Fluorescent microscope using Zen Imaging Software. Pictures were taken for 5 random locations on the slides at 2 different depths per location.

2.5.2 Macrophage Migration Assay

Macrophages were transfected with antimiR-92a and a control antimiR after 7 days of normal culture. The same transfection procedure as previously described was used for this experiment. After 48 hours of transfection, cells were serum starved with migration media (DMEM + 0.1% BSA; Sigma) for 1.5 hours in preparation for the migration assay. While cells were starving, the bottom migration plate (CIM-Plate 16) was prepped by adding 160μL of migration media with CCL2 (150ng/mL; R&D Systems) in the top 8 wells, and just migration media in the bottom 8 wells. The top chamber was then snapped on and an additional 30μL of migration media was added to all wells of the top chamber. The plate was then placed in the xCelligence RT Migration system (Roche) and placed in the incubator at 37^{o}C for 1 hour. After the transfected cells were lifted, counted, and resuspended at 2.0x10^{6} cells/mL. Prior to loading of the cells, the first step was ran on the prepped plate, just migration media and chemokine as previously describe, to calibrate for background. The plate was loaded with 2.0x10^{5} cells

(100μL) in each well. Each of the transfected cells were measured with and without CCL2 chemokine. After the cells were allowed to settle at room temperature for 30 minutes, the dual chamber plate was placed in the xCelligence machine at 37^{o}C. Measurements were taken every 5 minutes for 24 hours to obtain a comprehensive temporal profile of macrophage movement.

2.6 Statistical Analysis

Values are reported as mean±standard error. For western blot and qPCR analysis, data was reported as the mean fold-change of treatment to control. All data was analyzed with either a *t*-test or a one-way ANOVA. Probability values of $P<0.05$ were considered statistically significant.

Results

3. Results

3.1 Profiling Expression of miR-92a and Targets Post-MI

3.1.1 Collagen Matrix Alters the Expression Profile of miR-92a in the Post-MI Heart

It has been shown by our lab previously that injection of EDC/NHS crosslinked collagen is effective and improving revascularization and cardiac function while decreasing fibrosis and inflammation (Ahmadi et al., 2014; Blackburn et al., 2015). Given the anti-angiogenic and pro-inflammatory actions of miR-92a (Bonauer et al., 2009) and the significant down regulation of miR-92a at 2-days post-MI after matrix treatment (unpublished), it was hypothesized that injection of collagen matrix post-MI will result in a differential miR-92a expression profile. Mice underwent LAD ligation and were subsequently treated with nothing, PBS, or matrix at 3h post-MI. It was found that both PBS and matrix treated animals underwent a significant 35% and 75% down regulation of miR-92a, respectively at 4-hours post-injection compared to non-injected animals (Figure 2a). Additionally, miR-92a had significant reductions in matrix treated samples compared to PBS injected animals at 4-hours. At 1-day and 3-day post-injection, both PBS and matrix injected animals had significant reduction in miR-92a levels compared to non-treated animals with approximately 80% reduced expression (Figure 2a). There were no significant differences in miR-92a expression between PBS and matrix and 1 or 3-days. After 7d, miR-92a was upregulated 1.5-fold in PBS treated samples compared to non-treated samples, while matrix treated samples were 40% downregulated compared to PBS treated samples (Figure 2a).

3.1.2 Expression of miR-92a Targets in Cardiac Tissue Post-MI

Following up with miR-92a expression levels, the next goal was to determine how the expression of potential miR-92a targets was altered. First, a review of current literature as well as a search of databases was completed to identify predicted targets and pathways (TargetScan, miRDB, and miRSystem). RT-qPCR revealed that ITGAα5, a previously confirmed miR-92a target gene, was significantly upregulated at 3 and 7 days by 2.5-fold and 2.3-fold, respectively post-MI compared to PBS treatment. Additionally, ITGAα5 was upregulated at 3 and 7 days compared to 4-hour and 1-day matrix injected samples. A similar pattern was observed for another miR-92a target ITGAαV as 2-fold and 3-fold increased expression at 3 and 7-days were observed for matrix-treated hearts compared to PBS treated samples for those time points. When comparing time-points between matrix injected samples, ITGAαV expression at 3- and 7-day was upregulated compared to 4-hour and 1-day matrix injected samples. The anti-inflammatory S1Pr1 target was significantly upregulated by 3-fold at 7d post-MI in matrix treated cells compared to PBS treated at that time point, while also being upregulated compared to matrix treated samples at all other time points. Although SIRT1 expression in matrix-treated hearts weren't significantly different from PBS treated animals at any time point, it is upregulated by 1.7-fold at 1-day compared to the 4-hour matrix injected samples. STAT3 is an upstream regulator of miR-92a that may be a target for negative feedback (Lin et al., 2013). At 1-day, a 2.5-fold increase in expression was observed for matrix treated samples compared to the PBS group, while also being upregulated compared to matrix injected samples at 4-hour and 7-days post-injection. Furthermore, STAT3 expression in matrix injected samples collected at day 3 was upregulated 2-fold compared

to 7-day matrix treated samples. Expression of IL-10, a marker of M2 polarization, was also examined. Compared to PBS, there was a 2.9-fold upregulation of IL-10 in 3-day matrix samples, which was also significantly upregulated compared to matrix treated samples at all other time points. It should also be noted that there is a trend for IL-10 upregulation in matrix treated samples at 7-days post-MI vs. PBS.

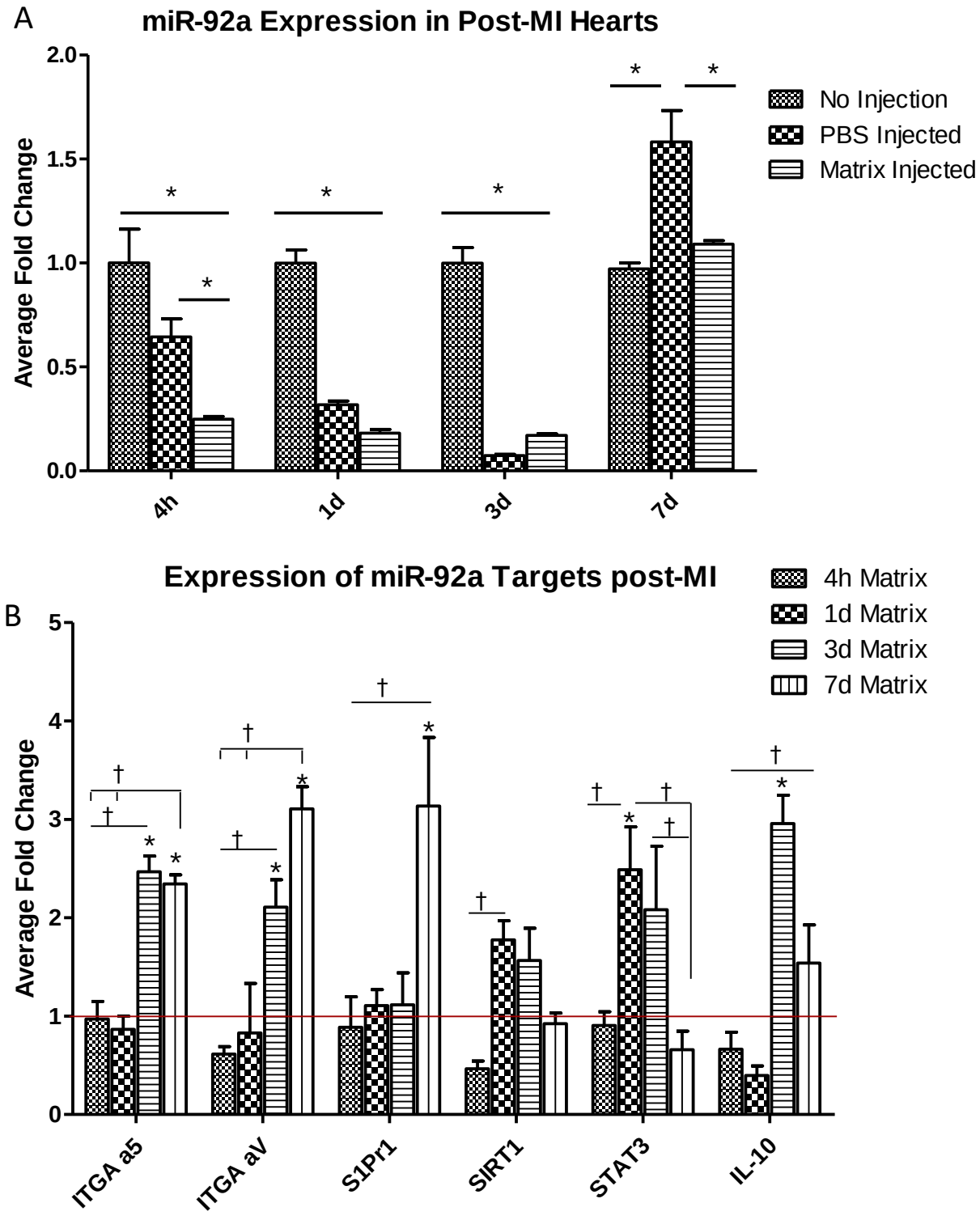

Figure 2. *In Vivo* expression of miR-92a and its targets in non-treated and treated infarcted hearts. A) Matrix treatment resulted in reduced miR-92a expression in MI

hearts at 4h and 7d compared to the PBS treatment group. Expression was calculated using RT-qPCR normalized to U6 and graphically compared to non-treated animals at each respected time point (n=3 for all time points). B) Matrix treatment significantly increased the expression of several potential miR-92a target genes at different time-points post-MI. The RT-qPCR data is presented as relative expression normalized to HPRT compared to PBS treated animals (depicted as the red line; n=3 for all time points). * Represents PBS vs Matrix for the respective time point, $p \leq 0.05$. † represents comparison between time-points for matrix injected samples, $p \leq 0.05$.

3.2 Matrix Alters Endogenous Expression of miR-92a in Macrophages *In Vitro*

Since it was shown that there was decreased miR-92a *in vivo* in matrix treated hearts and given that macrophages play an important role in MI healing (Blackburn et al., 2015; Frantz and Nahrendorf, 2014; Nahrendorf et al., 2007, 2010), *in vitro* cultures of bone marrow derived macrophages (BMDMs) were used to assess the ability of the matrix to mediate miR-92a in macrophages. BMDMs were cultured and plated on TCPS or matrix and allowed to adhere for 48h. It was found that cells cultured on matrix had 60% decreased miR-92a levels than cells grown on TCPS (Fig. 3a). Unfortunately, the RT-qPCR data for potential target gene expression was not as conclusive. Issues arising with RNA quality and matrix interacting with housekeeping genes failed to yield replicable data. However, at the protein level, western blot analysis revealed non-significant increased protein expression of S1Pr1 (1.3-fold; Fig. 3b) and SIRT1 (1.3-fold; Fig. 3c) in matrix cultured cells compared to TCPS cultured cells.

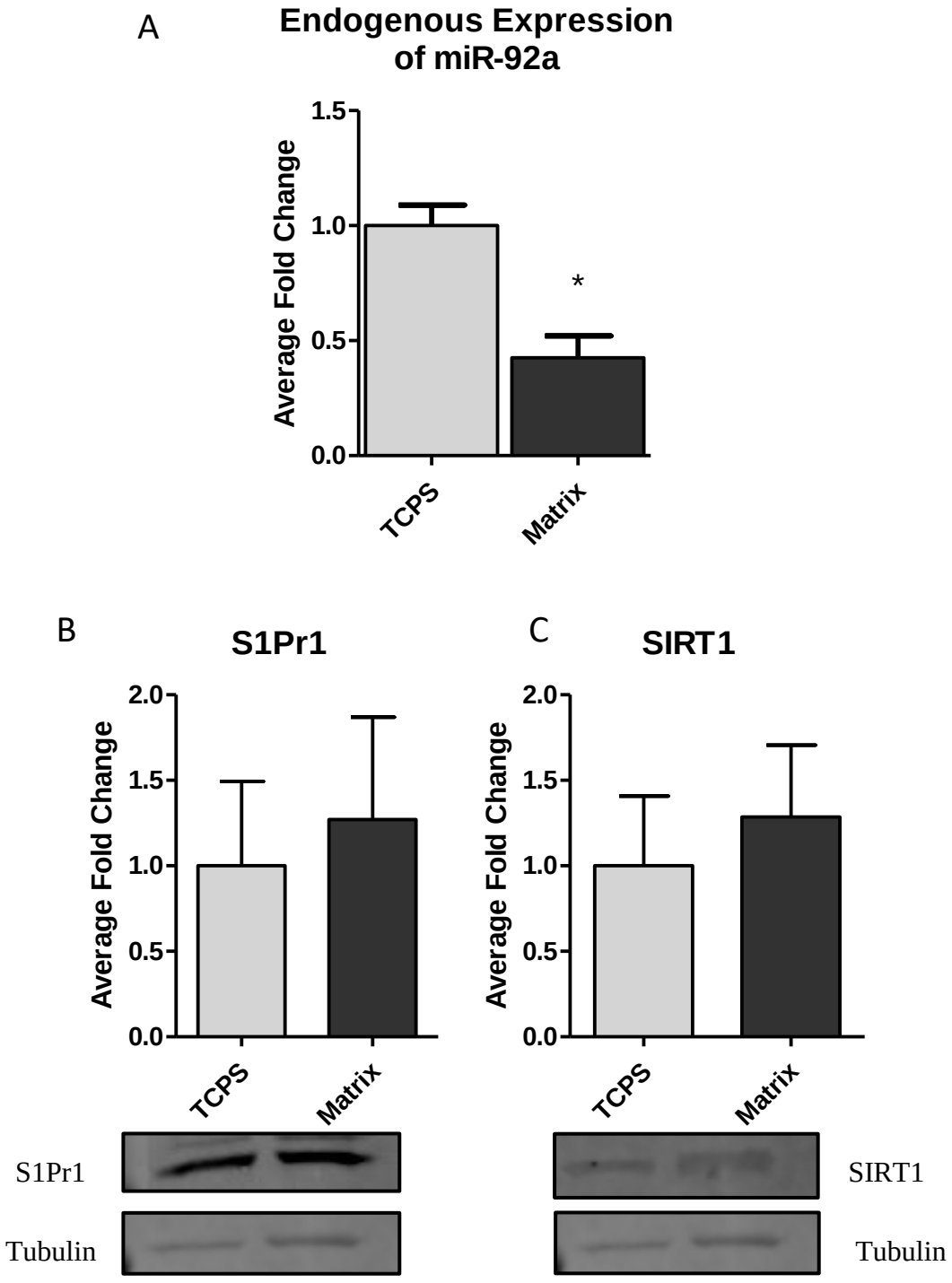

Figure 3. Endogenous Expression of miR-92a by Matrix and Protein Expression of Potential mRNA Targets. A) Reduction in miR-92a expression was observed in matrix

cultured BMDMs compared to TCPS ($p \leq 0.05$; n=3). B) S1Pr1 and C) SIRT1 protein expression following matrix culture ($p > 0.05$, n=3).

3.3 Induction and Inhibition of miR-92a Through Transfection

3.3.1 Inhibition of miR-92a causes Upregulation of Associated Targets

Due to the issues of obtaining reliable PCR data from matrix treated cells, antimiR treatment was implemented to mimic the endogenous down-regulation of miR-92a in macrophages with matrix treatment. BMDMs were cultured and treated with control antimiR or antimiR-92a for 48 hours prior to collection and analysis. miR-92a expression was reduced by 87% in antimiR treated cells compared to control cells (Fig. 4a) which is similar in magnitude to the levels of miR-92a downregulation by matrix. As hypothesized, there was an upregulation of all predicted targets in antimiR-92a treated cells compared to control treated cells (Fig. 4b). The adhesion molecules ITGA α5 and αV were upregulated 1.9- and 2.2-fold respectively compared to their control-miR transfected samples (Fig. 4b). Anti-inflammatory factor S1Pr1 was upregulated 2-fold, while SIRT1 had an increased expression of 2.3-fold compared to controls (Fig. 4b).

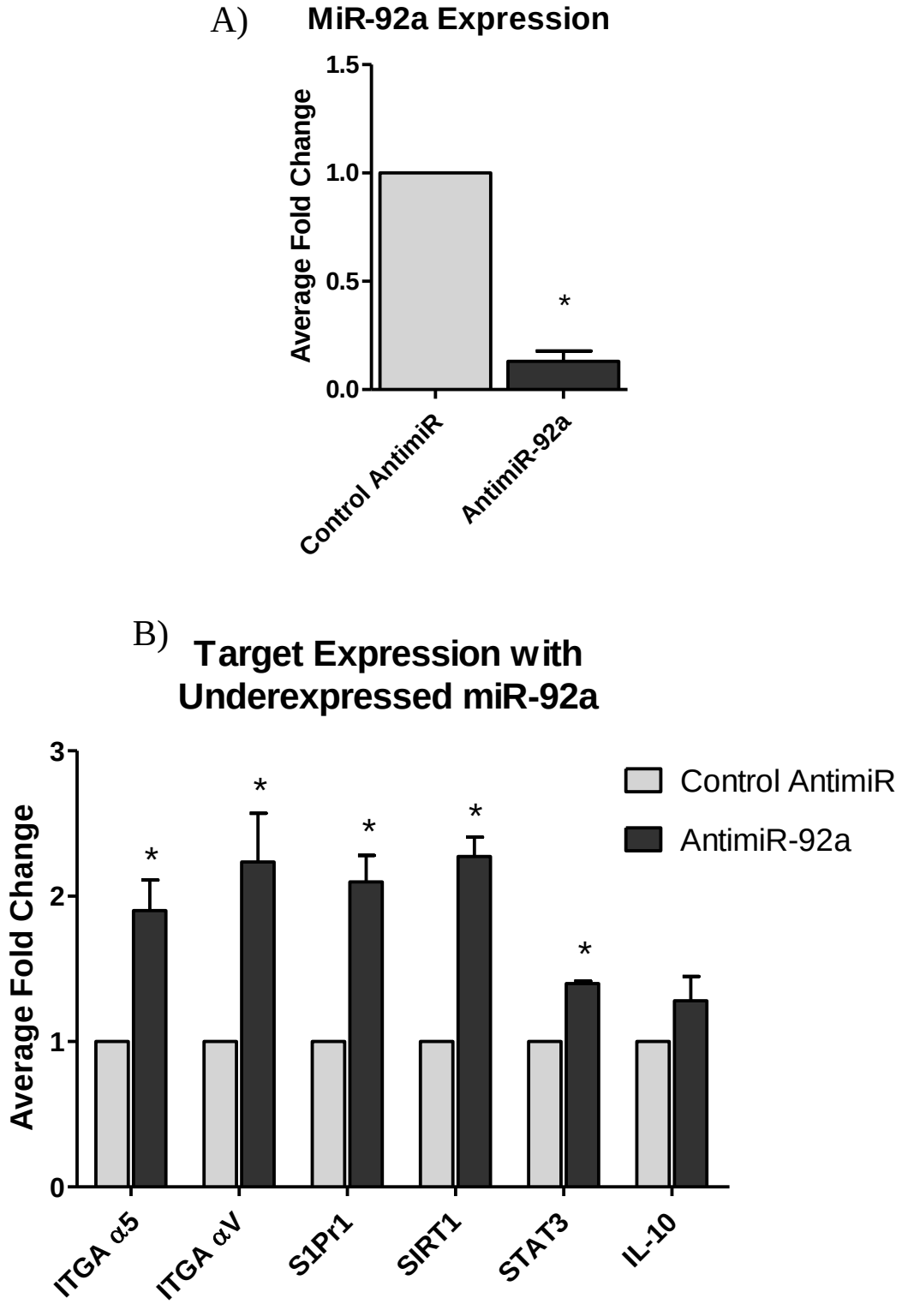

Figure 4. Expression of miR-92a and its targets in BMDMs treated with antimiR-92a. A) miR-92a expression is reduced in BMDMs following a 48-hour transfection with

antimiR-92a ($p \leq 0.05$, n=3). B) Upregulation of miR-92a targets in BMDMs treated with antimiR-92a compared to controls ($p \leq 0.05$, n=3). Data was analyzed using RT-qPCR normalized to U6 for miR-92a and 18s for targets, both compared to control treated cells.

3.3.2 Forced Over-Expression Results in Down-Regulation of Targets

In order to validate the miR-92a controls the expression of target genes in macrophages, forced over-expression of miR-92a was completed using miR-92a mimics. Transfection of BMDMs with miR-92a mimic resulted in a 33-fold upregulation in miR-92a expression compared to cells treated with control mimics (Fig. 5a). Incidentally, the increase in miR-92 resulted in significant target down-regulation ranging between 35-65% (Fig. 5b). ITGAα5 and S1Pr1 had the largest decrease in expression with 63% and 65% downregulation, respectively. ITGAαV was downregulated by 50% while SIRT1 had decreased expression by 35% compared to control samples. Western blot analysis was attempted; however, no quantifiable bands were detected in the mimic treatment group (possibly due to the drastic increase in miR-92a expression).

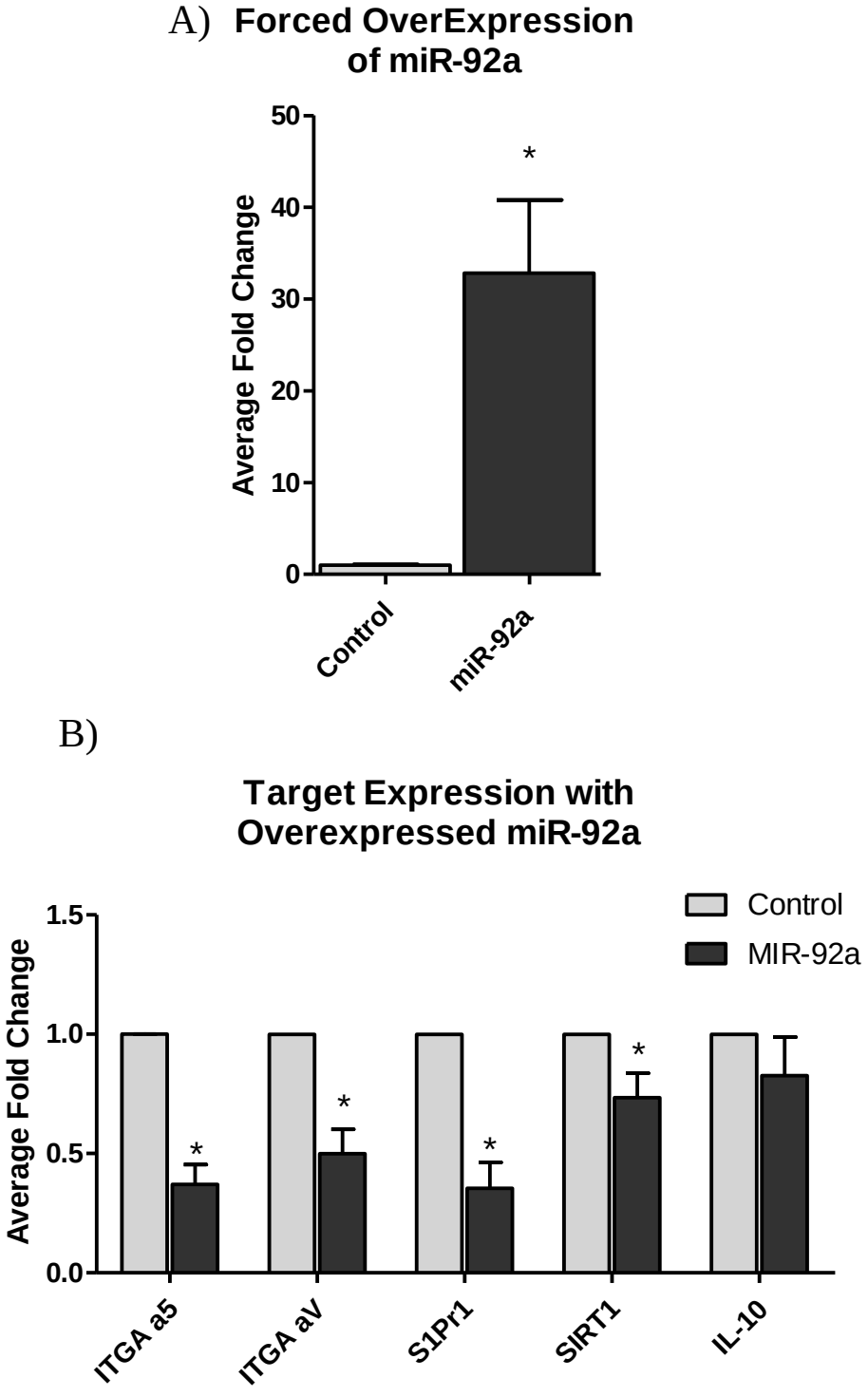

Figure 5. Expression of miR-92a and targets in BMDMs that overexpress miR-92a.

A) Expression of miR-92a following 48-hour transfection with miR-92a mimic compared

to cells treated with control mimic ($p \leq 0.05$, n=3). B) Increased ITGAα5, ITGAαV, S1Pr1 and SIRT1 expression in BMDMs following treatment with miR-92a mimic compared to control ($p \leq 0.05$, n=4). Data was analyzed using RT-qPCR normalized to U6 for miR-92a and 18s for targets, both compared to control treated cells.

3.4 Matrix Influence on Macrophage Adhesion and Migratory Function.

3.4.1 Macrophage Phenotypes Respond Differentially to Matrix

After determining that the miR-92a repression enhances expression of cell adhesion molecules ITGA α5 and αV, as well as anti-inflammatory factors S1Pr1 and SIRT1, we sought to determine how different macrophage phenotypes respond to matrix treatment (compared to standard TCPS culture). While no difference in miR-92a expression was observed in M0 macrophages between the substrates, it was found that matrix culture decreased its expression by 24% and 48% in M1 and M2 polarized macrophages, respectively (Fig. 6). Furthermore, M2 macrophages on matrix display a trend for reduced miR-92a expression compared to matrix-cultured M0 and M1 macrophages.

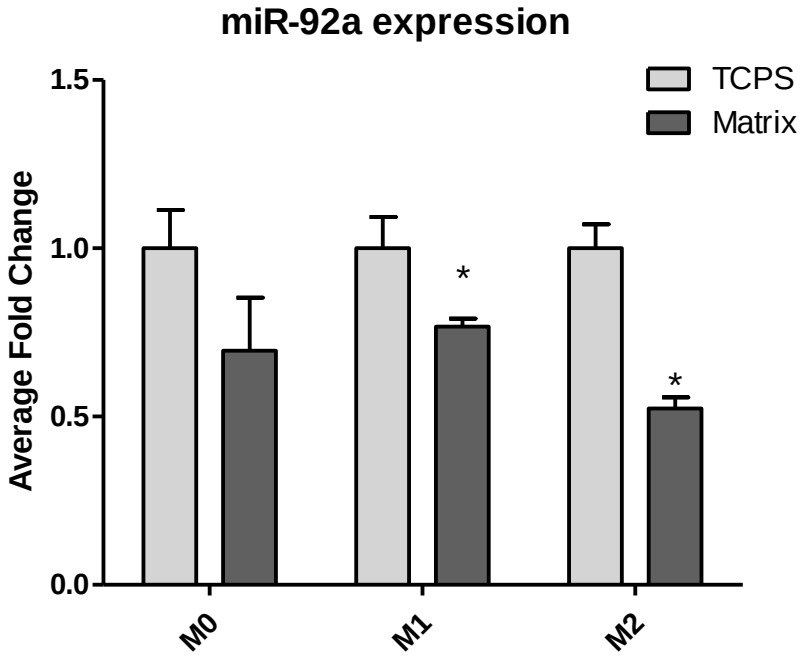

Figure 6. Expression of miR-92a in Different Macrophage Phenotypes Following TCPS or Matrix Culture. miR-92a expression is reduced in matrix treated M1 and M2 phenotypes compared to their respective TCPS controls. Expression was calculated using RT-qPCR normalized to U6 compared to TCPS cultures at the respective time point ($p \leq 0.05$, n=3 for all phenotypes).

3.4.2 Cellular Adhesion and Migration in Polarized Macrophages

Both ITGA α5 and αV are known to mediate cell interactions with the ECM as well as regulate cell migration. Since matrix treatment appears to influence anti-inflammatory functions, and M2 polarized macrophages had the largest decrease in miR-92a, it was hypothesized that M2 macrophages would better adhere to the matrix (possibly through increased ITGA α5 and αV expression). Polarized macrophages were stained with DAPI prior to seeding on matrix. Contrary to the hypothesis, there were no

significant differences in adhesion between any of the phenotypes (Fig. 7a). However, while taking initial pictures, 2 distinct planes of cells were identified within the matrix (Fig. 7b-g). By separately counting cells in the surface and deep planes, it was found that M0 cells had approximately equal number of cells at each depth. In contrast, there was a greater number of M1 macrophages at the surface compared to the number within the matrix; while M2 macrophages migrated and were more numerous deep within the matrix compared to the surface (Fig. 7h).

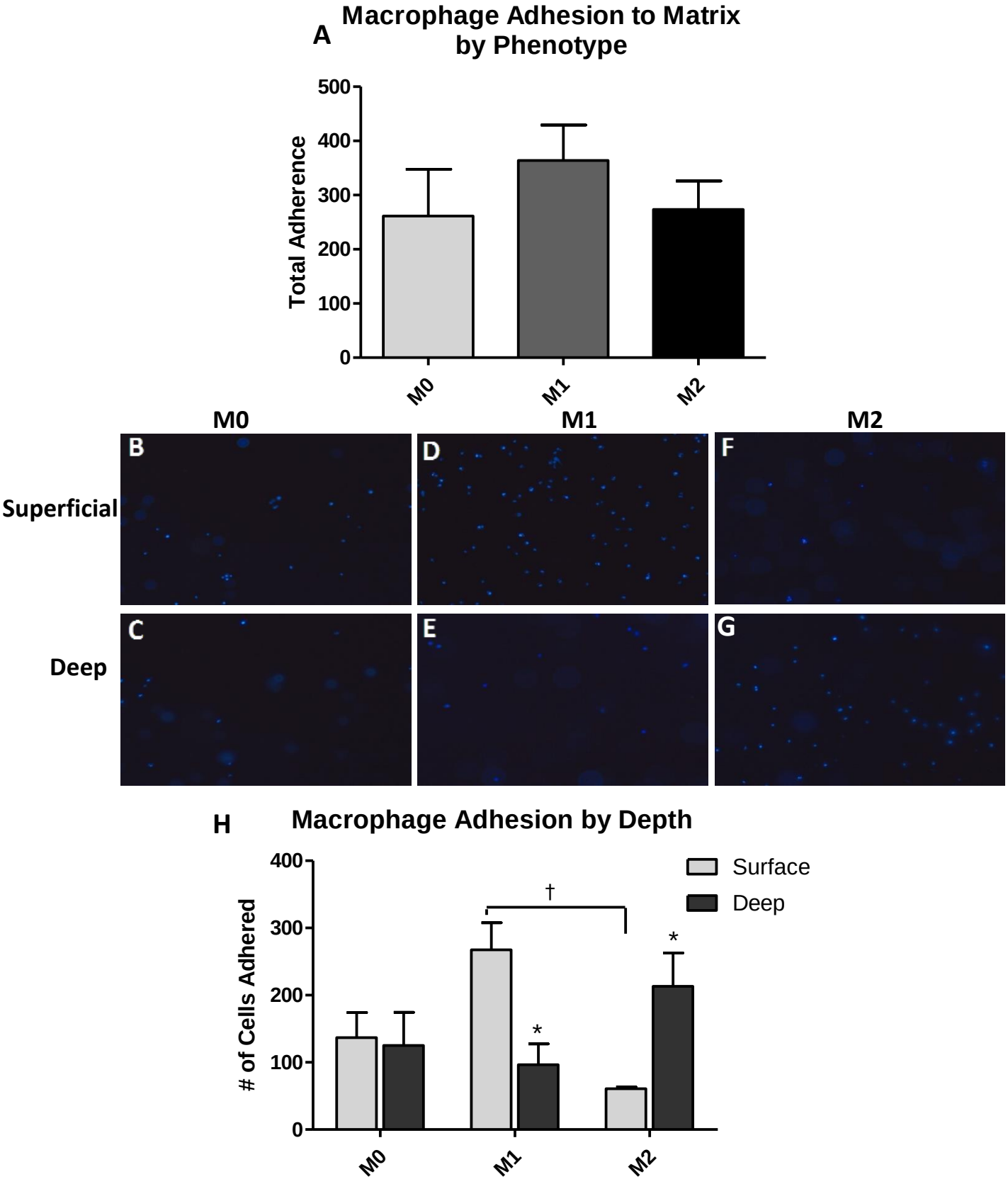
A
Macrophage Adhesion to Matrix by Phenotype
Total Adherence
500
400
300
200
100
0
M0
M1
M2
M0
M1
M2
Superficial
Deep
B
D
F
C
E
G
H
Macrophage Adhesion by Depth
# of Cells Adhered
400
300
200
100
0
Surface
Deep
†
*
*
M0
M1
M2

Figure 7. Matrix Effects on Adhesion and Migration of Different BMDM Phenotypes. A) Total adhesion of polarized macrophages to collagen matrix. B-G) Representative images of DAPI stained cells bound to matrix in different planes. Only distinct, focussed dot counted as cells; out of focus "clouds" not counted. H) Adhesion of polarized macrophages by depth in the matrix. Data presented as means of cells counted from 5 random FOV; $p \leq 0.05$, n=3). * Represents surface vs. deep within a phenotype, † represents comparison between different phenotypes, $p \leq 0.05$.

3.4.3 Effect of miR-92a on Macrophage Migration

Since BMDMs were observed to migrate into the matrix, we next attempted to further elucidate the role of miR-92a on macrophage migration. BMDMs were cultured for 6 days and then transfected with mimic or antimiR-92a and a control antimiR-92a or mimic. Cells were left to migrate in the xCelligence RT Migration System for 24h with measurements taken every 5 minutes. The raw data (Fig. 8a, 9a) were analyzed for area under the curve. Preliminary data reveals that inhibition of miR-92a leads to an increase in migration (Fig. 8b), whereas forced overexpression of miR-92a reduces macrophage migration (Fig. 9b).

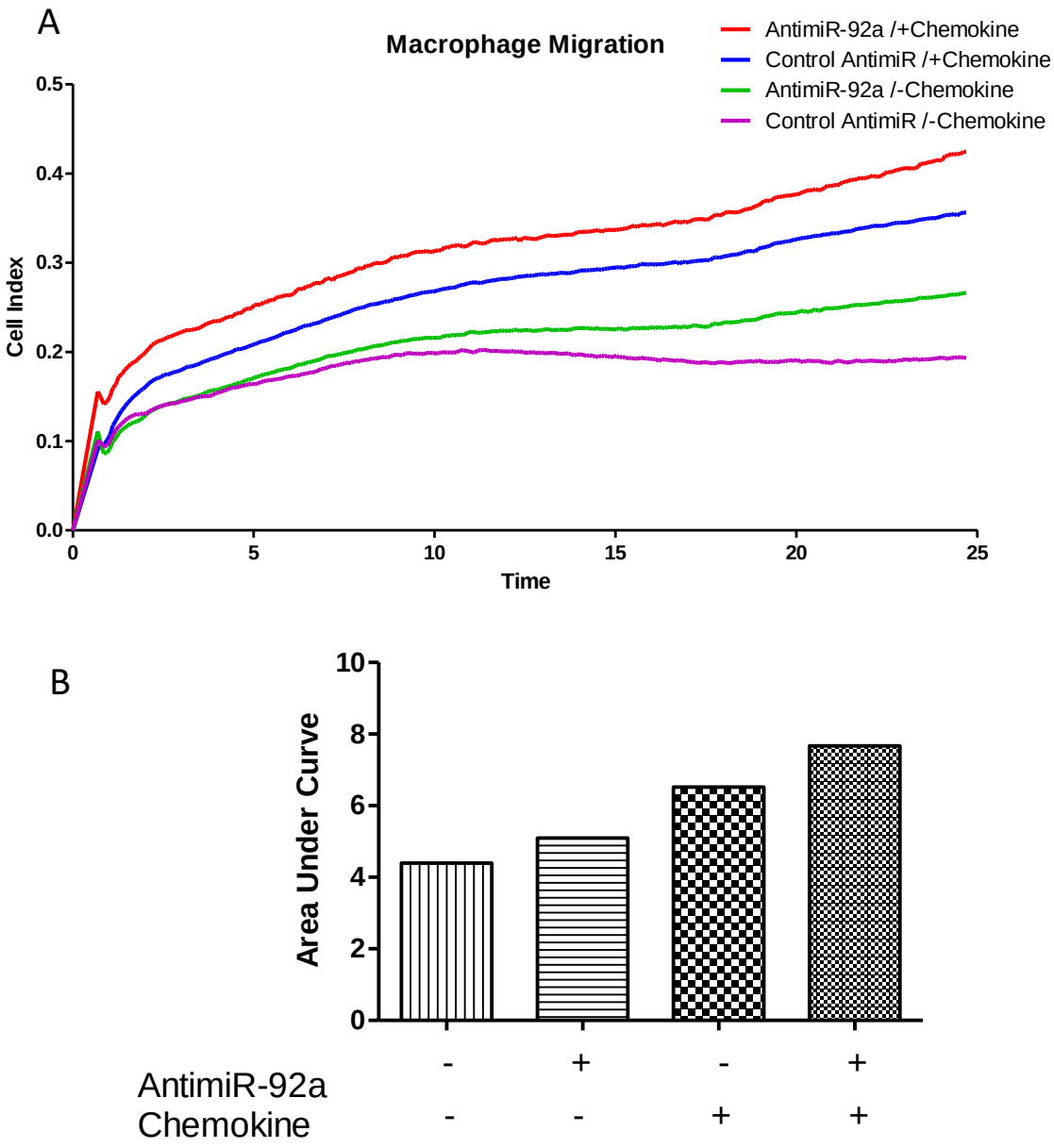

Figure 8. Inhibition of miR-92a promotes macrophage migration. A) Raw data of migration over a 24h period. B) Quantification of the area under the curve derived from the above data (n=1).

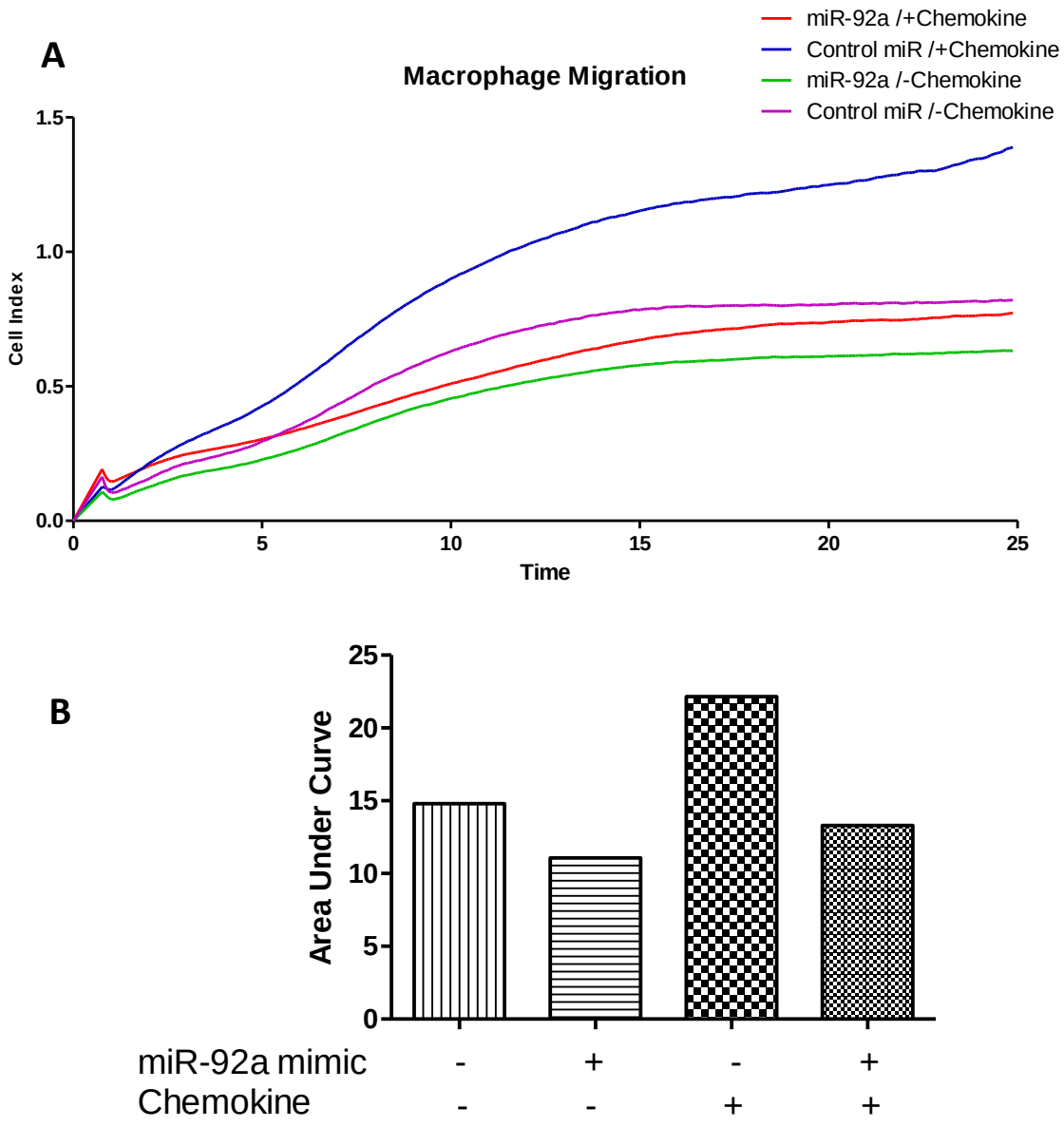

Figure 9. Forced overexpression of miR-92a impedes macrophage migration. C) Raw data of migration over a 24h period. D) Quantification of the area under the curve derived from the above data (n=1).

Discussion

4. Discussion

Following MI the heart undergoes extreme changes in its overall anatomical structure as well as its functional capacity. Current treatments focus on restoring blood flow followed by symptom alleviation which can prevent further loss of cardiac function, but it does not improve it. The complex nature of MI has made it difficult to develop treatments at the cell and molecular level that replace lost cells and/or improve the function of damaged cells. In previous pre-clinical studies, the injection of a EDC/NHS crosslinked collagen hydrogel has been able to increase LVEF and ventricular wall thickness, while reducing adverse remodelling (Ahmadi et al., 2014; Blackburn et al., 2015; Kuraitis et al., 2012). However, despite these results, the mechanism by which the matrix treatment exerts its therapeutic effect has remained elusive. Previous work in the lab revealed an altered miRNA expression profile in matrix-treated hearts at 2 days post-MI, which ultimately identified the pro-inflammatory and anti-angiogenic miR-92a to be of significant interest. The aim of this project was to further characterize the expression of miR-92a and some of its potential mRNA targets in the post-MI heart and determine if matrix treatment may be conferring some of its therapeutic benefit through the regulation of macrophage function via a miR-92a mechanism.

4.1 Matrix Treatment Alters Post-MI Microenvironment

4.1.1 Matrix Treatment Accelerates Inflammatory Healing Phase of MI through miR-92a Downregulation.

Previous work from the lab has shown that the injection of matrix at 3h post-MI leads to decreased inflammation in the myocardial tissue (Blackburn et al., 2015). MiR-

92a, which has been shown to be pro-inflammatory, is generally highly expressed following ischemic injury, including MI (Bonauer et al., 2009; Small et al., 2010). Matrix injected at 3h post-MI led to a significant reduction in miR-92a expression at 4h and 7d post-treatment, suggesting that miR-92a may be involved in the observed matrix benefits through the control of inflammation. Since miRNAs work through translational repression, meaning decreases in miRNA should lead to increases in target expression (Bartel, 2009; Nouraee and Mowla, 2015; O'Connell et al., 2010), we sought to profile the expression of several potential targets and regulators of miR-92a in the post-MI heart over time.

Despite significant decreases in miR-92a in matrix treated animals 4h post-injection compared to both PBS- and non-injected animals, there was no difference in the expression of any miR-92a targets at this time. In the early hours post-MI, the body is activating its initial responses and cellular activity is chaotic with mass necrosis and apoptosis (Deten et al., 2002; Fraccarollo et al., 2012; Frangogiannis, 2012; Sutton and Sharpe, 2015). One of the first events involves the upregulation of adhesion molecules on endothelial cells, which leads to the recruitment of phagocytic neutrophils, the first major immune cell to localize in the infarct and secrete inflammatory cytokines (Swirski and Nahrendorf, 2013). The rapid accumulation of neutrophils post-MI may have resulted in the consumption of previously upregulated adhesion molecules or their degradation as proteases are also prominent during this period which could explain the lack of expression at 4h and 1d post-MI. In the present study, S1Pr1 and SIRT1, which are both involved with anti-inflammatory pathways, were not upregulated at 4h post-treatment, as

would be expected since the infarct is filled with inflammatory neutrophils and CX_3CR1^+ monocytes (Jung et al., 2013; Swirski and Nahrendorf, 2013). Similarly, the expression of STAT3 and IL-10, both involved with M2 polarization and anti-inflammatory functions, was not increased early after matrix treatment.

No difference in miR-92a expression was observed at 1d post-MI between the PBS and matrix-treated mice, while its expression for both these groups was reduced compared to non-injected controls. We observed a significant increase in STAT3 expression in matrix treated hearts compared to PBS. Furthermore, for the matrix treatment, STAT3 levels were greater at 1d vs. the 4h and 7d time points. This may indicate an earlier resolution of the acute inflammatory phase, as STAT3 expression has been linked to cardioprotection (Fraccarollo et al., 2012; Haghikia et al., 2014; Hilfiker-Kleiner et al., 2004). Early relief of inflammation and the prevention of excess inflammatory events may be a key function of the matrix contributing to the improved LVEF, increased wall thickness, and reduced scar size observed in matrix treated groups (Ahmadi et al., 2014; Blackburn et al., 2015). Similar functional benefits have also been observed by Kobayashi et al and attributed to increased activation of STAT3 following injection with their erythropoietin-gelatin biomaterial (Kobayashi et al., 2008). Supporting the theory of early relief of inflammation is the marked increase in expression of IL-10 at 3d in matrix treated samples that we observed. IL-10 signaling reduces leukocyte infiltration (Frangogiannis, 2006), and in conjunction with elevated STAT3 levels, it is known to be a potent inducer of alternatively active, M2 macrophages (Krishnamurthy et al., 2009; Peda et al., 2016). In fact, previous reports profiling the

immune cells present in an infarct described days 3-5 as most prominently being M1, with M2 macrophages peaking at day 7 (Yan et al., 2013). The importance of IL-10 and STAT3 as regulators of M2 polarization was shown in a cyst cell microenvironment; increasing the level of IL-10 alone was not sufficient to change macrophage phenotype, however, sustained IL-10 leading to STAT3-mediated pathway activation promoted M2 polarization and the proliferation of cysts (Peda et al., 2016). In a relevant heart model, the injection of IL-10 following ischemia and reperfusion was demonstrated to be effective at alleviating inflammation and providing cardioprotection. It was determined that these effects were mediated through activation of STAT3, as IL-10 injected with Stattic (a STAT3 inhibitor) did not elicit the cardioprotective outcomes indicating IL-10 requires STAT3 for full anti-inflammatory results (Manukyan et al., 2011). Similarly, Krishnamurthy et al (2011) aimed to inhibit excessive post-MI inflammation by the administration of exogenous IL-10. It was found that IL-10 treatment significantly reduced infarcted myocardial inflammation 3 days post-MI accompanied by attenuation of ventricular dysfunction and wall thinning with reductions in infarct size at 14 and 28 days post-MI. In terms of IL-10 and STAT3 interactions, increased phosphorylated STAT3 (p-STAT3) was found at 3 and 28 days post-MI in IL-10 treated animals. The increase in p-STAT3 was associated with increased capillary density in the infarct potentially mediated through increased VEGF-A (Krishnamurthy et al., 2009). The ability of STAT3 to increase capillary density had previously been reported: STAT3 knockout mice had reduced myocardial capillary circulation and increased cardiac fibrosis after 4 months post-natal (Hilfiker-Kleiner et al., 2004). Interestingly, STAT3 has also been shown to play a role in the regulation of fibroblast activity (Hilfiker-Kleiner et

al., 2004; O'Sullivan et al., 2016). Based on this literature and results, and the increased STAT3 and IL-10 that was observed in response to matrix treatment, it is likely that the matrix is improving the post-MI microenvironment through macrophage polarization and reduction of inflammation, though further experiments need to be done to characterize present macrophages at this time.

STAT3 has also been reported to be involved in the proliferative phase of MI through the moderation of fibroblast activity. An increase in STAT3 expression has been shown to increase miR-21 which can target Spry1 and PTEN, known to be key mediators of cardiac fibrosis (Dong et al., 2014; Haghikia et al., 2014). Given that matrix treatment reduces fibrosis in the MI heart (Blackburn et al., 2015), it is possible that the matrix is activating STAT3 signaling in macrophages and fibroblasts. To determine activation status, it would be interesting to follow up with an expression profile of p-STAT3 to see if the STAT3, increased in response to matrix, is being phosphorylated. *In vitro* experiments should also be done with miR-92a and antimiR-92a transfected cell cultures to determine if miR-92a targets STAT3 directly of if increases are due to another matrix mediated mechanism. In addition, the expression of miR-21 should be looked at to determine if matrix benefits may be regulated through a STAT3-miR-21 mechanism.

The increase in SIRT1 we observed *in vivo* after matrix treatment may be a direct result of reduced miR-92a expression, as the same was seen in cultured macrophages after inhibition of miR-92a. The upregulation of SIRT1 has been found to have a protective effect against oxidative stress in retinal pigmented epithelium cells through

activation of JAK2/STAT3 signaling (Li et al., 2015). Early upregulation of this gene, in concert with the previously discussed targets supports the theory that matrix accelerates the healing process by early amelioration of the inflammatory phase. In macrophages, deletion of SIRT1 results in increased inflammation derived from M1 macrophages in liver and adipose tissue of mouse fed high fat diets (Ka et al., 2015; Yoshizaki et al., 2010). Another miR-92a target known to mediate macrophage function is the sphingosine-1-phosphate receptor, which was found to be upregulated at 7 days post-MI in matrix-treated hearts. Activation of this G protein coupled receptor by its S1P ligand leads to JAK2/STAT3 signaling providing cardioprotection through increased levels of p-STAT3 (Somers et al., 2012; Wang et al., 2016). Furthermore, pre-treatment of the MI heart with S1P can lead to increased nuclear and mitochondrial STAT3 levels culminating in a smaller infarct (Frias et al., 2012; Kelly-Laubscher et al., 2014). In macrophages specifically, activation of S1Pr1 led to a decrease in the secretion of pro-inflammatory cytokines TNFα, IL-12 and protein-1 from LPS-induced macrophages (Hughes et al., 2008). Activation of the M2 phenotype reduces cardiac inflammation and promotes constructive remodeling post-MI (Frantz and Nahrendorf, 2014; Nahrendorf et al., 2010). While there are many factors that may regulate macrophage differentiation and function, changes in miRNA expression are likely to play an important role. Control through miRNA mechanisms is complicated because genes are generally targeted by several miRNAs in many cell types. For example, miR-92a is known to target SIRT1 in macrophages; and in proangiogenic cells, miR-34a and miR-199a have been shown to mediate SIRT1 expression leading to detrimental vascular repair and cardiomyocyte apoptosis, respectively, following ischemic events (Seeger et al., 2013; Small et al.,

2010). Overall, early upregulation of SIRT1 and S1Pr1, in consort with the previously discussed miR-92a targets, supports the theory that the matrix accelerates the healing process through an earlier resolution of the inflammatory phase. However, further experimentation needs to be done to confirm that miR-92a is directly responsible for these effects.

4.1.2 Importance of Macrophages in Post-MI Wound Healing

Macrophages play a vital role in the initiation and remediation of any wound healing process. Highly plastic, macrophages have local populations of cells in many organs of the body such as Kupffer cells in the liver, alveolar macrophages in the lungs and foam cells in plaque to name a few (Zhang and Wang, 2014). Upon injury, macrophages are localized by tissue local macrophages and neutrophils through the secretion of pro-inflammatory cytokines and chemokines hours after the infarct (Lindsey et al., 2016; Nahrendorf et al., 2010). Monocytes converge on the infarcted tissue where they polarize to the pro-inflammatory M1 phenotype to further recruit inflammatory cells and undertake tasks such as debris clearance. This inflammatory process generally persists for a week post-MI (Frangogiannis, 2008; Nahrendorf and Swirski, 2013; Yan et al., 2013). Interestingly, after treatment with our matrix biomaterial, the expression patterns of SIRT1, IL-10, and STAT3 indicate transition from the inflammatory to the proliferation/maturation phases of MI. Work from other biomaterial labs have reported that macrophages respond to physical characteristics such as fiber diameter, fiber tension, and pore size, demonstrating macrophage responsiveness to biomaterial therapy (Garg et al., 2013; Wang et al., 2014). Biomaterials do require extensive testing as not all have

resulted in positive results when interacting with macrophage populations. For example, macrophages cultured on polyethylene terephthalate for 3 days resulted in increased M1:M2 ratios (Grotenhuis et al., 2013).

Indeed, initial inflammation is necessary to commence the healing process, however, M1 dysfunction contributes to excessive loss of cell mass, fibrosis, arrhythmia and subsequent heart failure (Francis Stuart et al., 2016). As the MI progresses, macrophages undergo a phenotypic transformation from a harmful inflammatory M1 phenotype, to the anti-inflammatory M2 macrophage. Macrophages with the M2 phenotype, in terms of infarct repair, are known to be beneficial leading to reduced adverse remodeling, and improvements in cardiac function parameters such as ejection fraction and end diastolic volume (Harel-Adar et al., 2011; Leor et al., 2016). M2 macrophages have distinctly different surface markers, such as Ly-6C^{Lo}, with different chemokine expression, which oppose that of M1 cells (Mantovani et al., 2004; Nahrendorf et al., 2007). The functions of M2 macrophages post-MI include the promotion of angiogenesis through the secretion of VEGF, influencing migration through secretion of MMPs, and production of TGF-β influencing myofibroblasts (Frantz and Nahrendorf, 2014; Zhang and Wang, 2014). It is possible that an M2-mediated mechanism may be playing a role in the increased angiogenesis and reduced fibrosis observed in matrix-treated MI hearts (Blackburn et al., 2015).

Along with influencing macrophage phenotype, down-regulation of miR-92a has also been linked to increases in migration (Daniel et al., 2014; Iaconetti et al., 2012), as

well as increased invasiveness of breast cancer (Nilsson et al., 2012). Cell migration is an important function for reparative cells to allow them to access the damaged tissue. *In vitro* it was shown that M2 polarized macrophages had decreased miR-92a when cultured on matrix compared to other phenotypes, which was qualitatively associated with increased migration. Preliminary quantitative data supported the qualitative observations as macrophages transfected with antimiR-92a had increased migration into the matrix. Increased M2 migration is desirable as this would enable cells to promote wound healing deeper within the tissue, that otherwise may have been inaccessible to macrophages. Several groups have demonstrated increased migration in mononuclear and fibroblast migration after treatment with biomaterial (Van Goethem et al., 2010; Piao et al., 2007; Raeber et al., 2007). However, no miRNA analysis was conducted to fully characterize the migration mechanism.

Macrophages have been known to partake in autocrine and paracrine signaling, which plays a large role in how M2 macrophages exert their positive effects. For example, it was previously shown that macrophages are required for endothelial tip vascular anastomosis in the hindbrain (Fantin et al., 2010). In a model of MI, dysfunctional macrophage signaling leads to the phenotypic conversion of fibroblasts to myofibroblasts and excess ECM deposition (Wynn and Vannella, 2016). As well as activating neighboring cells, IL-10 has been shown to bind its own surface receptor in an autocrine fashion to initiate JAK/STAT signaling in order to self-polarize to the cardioprotective M2 phenotype (Peda et al., 2016). Thus, matrix treatment of the MI

heart may be promoting such pro-healing M2 macrophage functions, which are crucial for cell-cell communication involved in mediating the healing process.

4.2 Interactions between the Collagen Matrix and Cell Adhesion Molecules

Cell adhesion molecules (CAMS) play an integral role in the post-MI environment facilitating cell-cell communication through ECM interactions. One family of CAMS that plays central role in the mediation of myocardial events is the integrin family. These particular CAMS are abundant in cardiac cells and contribute to migration, angiogenesis, mechanotransduction, and heart development (van der Flier et al., 2010; Ross and Borg, 2001). Of particular interest for this study are integrins α5 and αV, which are targets for regulation by miR-92a. Along with cellular interactions, integrins α5 and αV play a role in maintaining the extracellular environment through ECM homeostasis (Bornstein and Sage, 2002; Cho et al., 2016). Inhibition of ITG αV has been linked to the induction of pro-inflammatory gene expression and inflammation in atherogenic endothelial cells (Chen et al., 2015). miR-92a directly targets ITG α5 and αV, causing their down regulation reducing matrix interactions and angiogenic potential of cells (Anand, 2013; Bonauer and Dimmeler, 2009; Huang et al., 2014). In the present study, forced over expression of miR-92a in BMDMs *in vitro* led to significantly decreased expression of ITG α5 and αV mRNA. The opposite occurred in antimiR-92a treated cells, as ITG α5 and αV mRNA expression was increased. However, in BMDMs cultured with reduced miR-92a, western blot revealed negligible protein expression in matrix and control samples indicating integrins may not be highly expressed in the cultured macrophages. Alternatively, the collagenase treatment performed prior to cell lysis may

be damaging the integrin protein preventing its detection by the antibody, causing the appearance of low expression. Further troubleshooting of these methods could be performed, and/or the use of immunohistochemistry may provide information on integrin protein levels in BMDMs in response to interaction with the matrix.

Alterations in the native ECM can disrupt integrin binding resulting in substantial changes in cellular function. For example, during MI, excessive MMP production degrades large quantities of ECM subsequently cleaving integrin-collagen bonds disrupting pro-survival signaling (Chen et al., 2016; Rienks et al., 2014). Both ITG α5 and αV are verified direct targets of miR-92a; *in vitro,* forced over expression of miR-92a led to decreased expression of ITG α5 and αV in BMDMs. The opposite occurred in antimiR-92a treated cells. *In vivo* there was a significant increase in ITG α5 and αV expression at 3 and 7 days post-MI coinciding with decreased miR-92a expression compared to non-injected and PBS controls, respectively. Previous work from our group determined that matrix treatment increases integrin α2, α5 and αV expression in circulating angiogenic cells leading to increased adhesion, migration and angiogenic potential (Ahmadi et al., 2014; Mcneill et al., 2015). Bonauer et al. (2009) found that treatment of an ischemic hindlimb with anti-miR-92a led to significantly more angiogenesis attributed to increased ITG α5 and αV in endothelial cells. In fibroblasts, reductions of integrins α5 and results in decreased fibroblast migration (Almeida et al., 2016). Endothelial cells and fibroblasts play an integral role in the in healing the infarcted myocardium and are necessary for revascularization and scar formation, respectively.

Further research needs to be done on the role of macrophages in the influence of integrins to better understand potential targets for therapy.

4.3 MiRNAs and Cardiovascular Disease: Friend or Foe?

The role that miRNA plays in the pathology and prevention of disease is very complex and a growing field of research. Several miRNAs are well characterized regarding their role in the progression of cardiovascular disease. The dysregulation of over 65 miRNAs have been implicated in various stages of cardiovascular disease and in cardiac conditions such as stable and unstable angina, ST elongated MI (STEMI), and acute MI (Ahlin et al., 2016; Bostjancic et al., 2009; Small et al., 2010). Included in the list of identified miRNAs is the miR-17-92 cluster which includes miR-17 with roles in endothelial cell proliferation and miR-92a which is known for its previously discussed pro-inflammatory and anti-angiogenic effects on cardiac tissues (Bonauer and Dimmeler, 2009; Ranji et al., 2013). Matrix treatment downregulates miR-92a which leads to increased expression of anti-inflammatory and pro-angiogenic targets. Given the observed changes in miRNA expression, advances in the tracking of miRNAs may allow them to be used as biomarkers for disease. However, with high person-to-person variability, normalization would have large ranges and may not be conclusive. Although, miRNAs could be tracked on an individual basis and utilized as a response to therapy or predictor of who may benefit from alternative therapies.

Macrophages play an integral role in the mediation of many conditions. miRNAs take advantage of this in order promote the healing or pathology of disease. miRNA of

interest, miR-33 targets macrophages in the atherosclerotic plaque, suppressing the ABCA1 cholesterol transporter leading to the accumulation of HDL within cells. Further inhibition of miR-33 resulted in mobilization of ABCA1 and reversal of plaque progression by the efflux of HDL cholesterol into the plasma (Rayner et al., 2011). MiR-33 has also been shown to induce the prohealing-M2 macrophage phenotype (Karunakaran et al., 2015). Recently, miR-223 has been link to MI through its ability to ameliorate necroptosis in macrophages. Myocardial infarction in mice transgenic for pre-miR-223 had increase expression of miR-233 in cardiac tissue which resulted in the suppression of the inflammatory RIP1-R1P3-MLKL pathway leading to reduced necroptosis and cell survival (Qin et al., 2016). MiR-92a targets macrophage inflammatory pathways post-MI which result in increased cell death and excessive inflammation. Future work should focus on the pathway by which miR-92a functions in macrophages for specific treatment development.

Due to a miRNAs ability to target many processes in a variety of cell types, changing miRNA expression may have benefits in one part of the body, and simultaneously lead to the exacerbation of disease in another part of the body. In a cardio-specific example, miR-155 is associated with both endothelial cell tube formation and angiogenesis, as well as in macrophage induction of arteriogenesis. At a glance both sound beneficial, however, upon further inspection low levels miR-155 preferentially activate endothelial cells for microvessel angiogenesis. At high levels, arteriogenesis dominates. With implications miR-155 leading to the progression of atherosclerosis, thus increasing expression post-MI to regenerate major vessels may cause the exacerbation of

the atherosclerotic plaque resulting the contribution of further vessel occlusions (Rayner, 2015). Atherosclerosis and myocardial infarction generally go hand in hand, thus highlighting the necessity for balance in considering miRNA therapeutics. In terms of MI, indeed, decreasing miR-92a would appear to have a beneficial effect in the amelioration of MI, yet further research needs to be done to determine the comprehensive effects of miR-92a. An example of this is the function of miR-92a in the heart and in numerous cancers. It is well noted that inhibition of miR-92a results in the favorable increase of angiogenesis, migration, and cardioprotection for reperfusion injury (Bonauer et al., 2009; Daniel et al., 2014; Hinkel et al., 2013; Iaconetti et al., 2012). However, inhibition of miR-92a has been associated with increased invasiveness and metastasis of breast cancer (Nilsson et al., 2012), and the development of hepatocellular carcinoma (Shigoka et al., 2010). This is an important consideration for the aging population, as elderly people commonly present in the emergency room with multiple conditions. To address this, biomaterials can provide an approach to deliver localized treatment. Matrix treatment alone has already demonstrated the ability to regulate miR-92a expression. Future work should include incorporation of antimiR-92a into the biomaterial to of localized delivery to the infarct which would minimize off-target effects, and potentially result in further reduction of miR-92a and superior functional outcomes infarcted myocardium.

There needs to be further research done to profile miRNA in early, middle and late stages of disease to fully grasp how miRNA exert their effects on cellular pathways to know whether they are helping or harming. Mounting evidence demonstrates that miR-

92a is damming to effective cardiac regeneration whereas increasing levels of different miRNAs, such as miR-7a/b may increase regenerative potential (Li et al., 2016). The nature of miRNA in the pathogenesis or treatment of cardiovascular disease depends on the miRNA and the disease model at hand.

4.4 Future Directions

As an important next step, we should focus on optimization and repetition of the xCelligence migration study to confirm the role of miR-92a in the superior migration of anti-inflammatory M2 macrophages compared to pro-inflammatory M1 macrophages. It would also be beneficial to obtain protein expression levels in cells treated with antimiR-92a to confirm functionality of our selected miR-92a targets.

The next big picture step would be to determine the primary source or site of activity for miR-92a in the infarcted heart as well as the mechanism by which matrix treatment reduces its expression. To determine the cell type(s) in which miR-92a is found, myocardial tissue sections from MI hearts should be prepared for fluorescent in situ hybridization (FISH) by RNAscope. By doing this, specific cell types could be labeled with one probe and miR-92a could be labeled with a second probe; then overlapping consecutive images would identify the cell types containing intracellular miR-92a. Given that miRNAs can be packaged into exosomes for uptake by other cells, FISH analysis would provide information on where miR-92a is present at a specific time-point post-MI, but may not conclusively identify the cell that produced it. FISH analysis at different time-points post-MI would help to elucidate the cells generating miR-92a,

and whether signaling through exosomes may be a mechanism in the MI heart. Identifying how matrix treatment is effective at reducing miR-92a expression would require further database analysis to determine upstream regulators and activators of the *cl31orf25* gene and whether they are altered by matrix treatment. Another beneficial experiment would be to better determine how miR-92a influences the phenotype of macrophages. This could be done through mutation of known 3'UTRs of targets to incorporate green fluorescent protein (GFP) to be used in time course studies. Reduction of green fluorescence would indicate binding of miR-92a, then further pathway analysis of proteins could be done to elucidate the mechanism by which macrophage polarization is altered.

Conclusion

5. Conclusion

In conclusion, this study determined that matrix treatment alters the expression of miR-92a and its targets in the post-MI environment. Specifically, reduced miR-92a levels in matrix-treated hearts was associated with increased expression of IL-10, STAT3, SIRT1, S1Pr1, ITG α5 and ITG αV, which are involved in anti-inflammatory pathways or cell-ECM interactions. *In vitro* studies suggest that M2 macrophages are more responsive to matrix treatment as they had the greatest decrease in miR-92a, which was associated with increased migration on matrix. In summary, we report that the beneficial effects of matrix treatment post-MI may be mediated, at least in part, through its ability to regulate miR-92a and pro-wound healing mechanisms in macrophages. These results present the matrix as a novel non-pharmacological approach to locally regulate miRNAs *in vivo* for reducing inflammation and protecting the myocardium post-MI.

6. References

Ahlin, F., Arfvidsson, J., Vargas, K. G., Stojkovic, S., Huber, K., and Wojta, J. (2016). MicroRNAs as circulating biomarkers in acute coronary syndromes: A review. *Vascul. Pharmacol.* 81, 15–21. doi:10.1016/j.vph.2016.04.001.

Ahmadi, A., McNeill, B., Vulesevic, B., Kordos, M., Mesana, L., Thorn, S., et al. (2014). The role of integrin α2 in cell and matrix therapy that improves perfusion, viability and function of infarcted myocardium. *Biomaterials* 35, 4749–58. doi:10.1016/j.biomaterials.2014.02.028.

Almeida, M. E. S., Monteiro, K. S., Kato, E. E., Sampaio, S. C., Braga, T. T., Câmara, N. O. S., et al. (2016). Hyperglycemia reduces integrin subunits alpha v and alpha 5 on the surface of dermal fibroblasts contributing to deficient migration. *Mol. Cell. Biochem.* doi:10.1007/s11010-016-2780-4.

Ambros, V. (2004). The functions of animal microRNAs. *Nature* 431, 350–5. doi:10.1038/nature02871.

Anand, S. (2013). A brief primer on microRNAs and their roles in angiogenesis. *Vasc. Cell* 5, 2. doi:10.1186/2045-824X-5-2.

Antman, E. M., Anbe, D. T., Armstrong, P. W., Bates, E. R., Green, L. A., Hand, M., et al. (2004). *ACC/AHA Guidelines for the Management of Patients With ST-Elevation Myocardial Infarction--Executive Summary: A Report of the American College of Cardiology/American Heart Association Task Force on Practice Guidelines (Writing Committee to Revise the 1999*. doi:10.1161/01.CIR.0000134791.68010.FA.

Baltimore, D., Boldin, M. P., O'Connell, R. M., Rao, D. S., and Taganov, K. D. (2008). MicroRNAs: new regulators of immune cell development and function. *Nat. Immunol.* 9, 839–45. doi:10.1038/ni.f.209.

Bartel, D. P. (2004). MicroRNAs: Genomics, Biogenesis, Mechanism, and Function. *Cell* 116, 281–297. doi:10.1016/S0092-8674(04)00045-5.

Bartel, D. P. (2009). MicroRNAs: target recognition and regulatory functions. *Cell* 136, 215–33. doi:10.1016/j.cell.2009.01.002.

Bayomy, A. F., Bauer, M., Qiu, Y., and Liao, R. (2012). Regeneration in heart disease-Is ECM the key? *Life Sci.* 91, 823–7. doi:10.1016/j.lfs.2012.08.034.

Biernacka, A., and Frangogiannis, N. G. (2011). Aging and Cardiac Fibrosis. *Aging Dis.* 2, 158–173. doi:10.1016/j.bbi.2008.05.010.

Blackburn, N. J. R., Sofrenovic, T., Kuraitis, D., Ahmadi, A., McNeill, B., Deng, C., et al. (2015). Timing underpins the benefits associated with injectable collagen biomaterial therapy for the treatment of myocardial infarction. *Biomaterials* 39, 182–92. doi:10.1016/j.biomaterials.2014.11.004.

Bonauer, A., Carmona, G., Iwasaki, M., Mione, M., Koyanagi, M., Fischer, A., et al. (2009). MicroRNA-92a controls angiogenesis and functional recovery of ischemic tissues in mice. *Science* 324, 1710–3. doi:10.1126/science.1174381.

Bonauer, A., and Dimmeler, S. (2009). The microRNA-17~92 cluster: Still a miRacle? *Cell Cycle* 8, 3866–3873. doi:10.4161/cc.8.23.9994.

van den Borne, S. W. M., Diez, J., Blankesteijn, W. M., Verjans, J., Hofstra, L., and Narula, J. (2010). Myocardial remodeling after infarction: the role of myofibroblasts. *Nat. Rev. Cardiol.* 7, 30–37. doi:10.1038/nrcardio.2009.199.

Bornstein, P., and Sage, E. H. (2002). Matricellular proteins: Extracellular modulators of

cell function. *Curr. Opin. Cell Biol.* 14, 608–616. doi:10.1016/S0955-0674(02)00361-7.

Bostjancic, E., Zidar, N., and Glavac, D. (2009). MicroRNA microarray expression profiling in human myocardial infarction. *Dis. Markers* 27, 255–268. doi:10.3233/DMA-2009-0671.

Brown, B. N., Londono, R., Tottey, S., Zhang, L., Kukla, K. a., Wolf, M. T., et al. (2012). Macrophage phenotype as a predictor of constructive remodeling following the implantation of biologically derived surgical mesh materials. *Acta Biomater.* 8, 978–987. doi:10.1016/j.actbio.2011.11.031.

Lo Celso, C., and Scadden, D. T. (2011). The haematopoietic stem cell niche at a glance. *J. Cell Sci.* 124, 3529–3535. doi:10.1242/jcs.074112.

Chen, C., Li, R., Ross, R. S., and Manso, A. M. (2016). Integrins and integrin-related proteins in cardiac fibrosis. *J. Mol. Cell. Cardiol.* 93, 162–174. doi:10.1016/j.yjmcc.2015.11.010.

Chen, J., Green, J., Yurdagul, A., Albert, P., McInnis, M. C., and Orr, A. W. (2015). αvβ3 Integrins Mediate Flow-Induced NF-κB Activation, Proinflammatory Gene Expression, and Early Atherogenic Inflammation. *Am. J. Pathol.* 185, 2575–2589. doi:10.1016/j.ajpath.2015.05.013.

Cho, I., Jackson, M. R., and Swift, J. (2016). Roles of Cross-Membrane Transport and Signaling in the Maintenance of Cellular Homeostasis. *Cell. Mol. Bioeng.* 9, 234–246. doi:10.1007/s12195-016-0439-6.

Chong, J. J. H., Chandrakanthan, V., Xaymardan, M., Asli, N. S., Li, J., Ahmed, I., et al. (2011). Adult Cardiac-Resident MSC-like Stem Cells with a Proepicardial Origin. *Cell Stem Cell* 9, 527–540. doi:10.1016/j.stem.2011.10.002.

Daniel, J. M., Penzkofer, D., Teske, R., Dutzmann, J., Koch, A., Bielenberg, W., et al. (2014). Inhibition of miR-92a improves re-endothelialization and prevents neointima formation following vascular injury. *Cardiovasc. Res.* 103, 564–572. doi:10.1093/cvr/cvu162.

Deten, A., Volz, H. C., Briest, W., and Zimmer, H.-G. (2002). Cardiac cytokine expression is upregulated in the acute phase after myocardial infarction. Experimental studies in rats. *Cardiovasc. Res.* 55, 329–340. doi:S0008636302004133 [pii].

Dewald, O. (2005). CCL2/Monocyte Chemoattractant Protein-1 Regulates Inflammatory Responses Critical to Healing Myocardial Infarcts. *Circ. Res.* 96, 881–889. doi:10.1161/01.RES.0000163017.13772.3a.

Dobaczewski, M., Gonzalez-Quesada, C., and Frangogiannis, N. G. (2011). The extracellular matrix as a modulator of the inflammatory and reparative response following myocardial infarction. *J. Mol. Cell. Cardiol.* 48, 504–511. doi:10.1016/j.yjmcc.2009.07.015.The.

Dong, S., Cheng, Y., Yang, J., Li, J., Liu, X., Wang, X., et al. (2009). MicroRNA expression signature and the role of microRNA-21 in the early phase of acute myocardial infarction. *J. Biol. Chem.* 284, 29514–25. doi:10.1074/jbc.M109.027896.

Dong, S., Ma, W., Hao, B., Hu, F., Yan, L., Yan, X., et al. (2014). microRNA-21 promotes cardiac fibrosis and development of heart failure with preserved left ventricular ejection fraction by up-regulating Bcl-2. *Int. J. Clin. Exp. Pathol.* 7, 565–

574.
Dorn, G. W. (2011). MicroRNAs in cardiac disease. *Transl. Res.* 157, 226–35. doi:10.1016/j.trsl.2010.12.013.
Dzau, V. J., Antman, E. M., Black, H. R., Hayes, D. L., Manson, J. E., Plutzky, J., et al. (2006). The cardiovascular disease continuum validated: Clinical evidence of improved patient outcomes: Part I: Pathophysiology and clinical trial evidence (risk factors through stable coronary artery disease). *Circulation* 114, 2850–2870. doi:10.1161/CIRCULATIONAHA.106.655688.
Ehninger, A., and Trumpp, A. (2011). The bone marrow stem cell niche grows up: mesenchymal stem cells and macrophages move in. *J. Exp. Med.* 208, 421–428. doi:10.1084/jem.20110132.
Fan, D., Creemers, E. E., and Kassiri, Z. (2014). Matrix as an interstitial transport system. *Circ. Res.* 114, 889–902. doi:10.1161/CIRCRESAHA.114.302335.
Fantin, A., Vieira, J. M., Gestri, G., Denti, L., Schwarz, Q., Prykhozhij, S., et al. (2010). Tissue macrophages act as cellular chaperones for vascular anastomosis downstream of VEGF-mediated endothelial tip cell induction. *Blood* 116, 829–840. doi:10.1182/blood-2009-12-257832.
van der Flier, A., Badu-Nkansah, K., Whittaker, C. a, Crowley, D., Bronson, R. T., Lacy-Hulbert, A., et al. (2010). Endothelial alpha5 and alphav integrins cooperate in remodeling of the vasculature during development. *Development* 137, 2439–2449. doi:10.1242/dev.049551.
Fraccarollo, D., Galuppo, P., and Bauersachs, J. (2012). Novel therapeutic approaches to post-infarction remodelling. *Cardiovasc. Res.* 94, 293–303. doi:10.1093/cvr/cvs109.
Francis Stuart, S. D., De Jesus, N. M., Lindsey, M. L., and Ripplinger, C. M. (2016). The crossroads of inflammation, fibrosis, and arrhythmia following myocardial infarction. *J. Mol. Cell. Cardiol.* 91, 114–122. doi:10.1016/j.yjmcc.2015.12.024.
Frangogiannis, N. G. (2006). The Mechanistic Basis of Infarct Healing. *Antioxid. Redox Signal.* 10, 1907–1939. doi:10.1089/ars.2007.1957.
Frangogiannis, N. G. (2008). The immune system and cardiac repair. *Pharmacol. Res.* 58, 88–111. doi:10.1016/j.phrs.2008.06.007.
Frangogiannis, N. G. (2012). Regulation of the Inflammatory Response in Cardiac Repair. *Circ. Res.* 110, 159–173. doi:10.1161/CIRCRESAHA.111.243162.
Frangogiannis, N. G., Mendoza, L. H., Ren, G., Akrivakis, S., Jackson, P. L., Michael, L. H., et al. (2003). MCSF expression is induced in healing myocardial infarcts and may regulate monocyte and endothelial cell phenotype MCSF expression is induced in healing myocardial infarcts and may regulate monocyte and endothelial cell phenotype. *Am. J. Phys. Hear. Circ. Physiol.* 285, 483–492. doi:10.1152/ajpheart.01016.2002.
Frantz, S., and Nahrendorf, M. (2014). Cardiac macrophages and their role in ischaemic heart disease. *Cardiovasc. Res.* 102, 240–248. doi:10.1093/cvr/cvu025.
Frias, M. A., Lecour, S., James, R. W., and Pedretti, S. (2012). High density lipoprotein/sphingosine-1-phosphate-induced cardioprotection: Role of STAT3 as part of the SAFE pathway. *Jak-Stat* 1, 92–100. doi:10.4161/jkst.19754.
Garg, K., Pullen, N. a., Oskeritzian, C. a., Ryan, J. J., and Bowlin, G. L. (2013). Macrophage functional polarization (M1/M2) in response to varying fiber and pore dimensions of electrospun scaffolds. *Biomaterials* 34, 4439–4451.

doi:10.1016/j.biomaterials.2013.02.065.
Van Goethem, E., Poincloux, R., Gauffre, F., Maridonneau-Parini, I., and Le Cabec, V. (2010). Matrix architecture dictates three-dimensional migration modes of human macrophages: differential involvement of proteases and podosome-like structures. *J. Immunol.* 184, 1049–1061. doi:10.4049/jimmunol.0902223.
Gong, C., Nie, Y., Qu, S., Liao, J. Y., Cui, X., Yao, H., et al. (2014). miR-21 induces myofibroblast differentiation and promotes the malignant progression of breast phyllodes tumors. *Cancer Res.* 74, 4341–4352. doi:10.1158/0008-5472.CAN-14-0125.
Gordon, S. (2003). Alternative activation of macrophages. *Nat. Rev. Immunol.* 3, 23–35. doi:10.1038/nri978.
Grotenhuis, N., Bayon, Y., Lange, J. F., Van Osch, G. J. V. M., and Bastiaansen-Jenniskens, Y. M. (2013). A culture model to analyze the acute biomaterial-dependent reaction of human primary macrophages. *Biochem. Biophys. Res. Commun.* 433, 115–120. doi:10.1016/j.bbrc.2013.02.054.
Haghikia, A., Ricke-Hoch, M., Stapel, B., Gorst, I., and Hilfiker-Kleiner, D. (2014). STAT3, a key regulator of cell-to-cell communication in the heart. *Cardiovasc. Res.* 102, 281–289. doi:10.1093/cvr/cvu034.
Harel-Adar, T., Ben Mordechai, T., Amsalem, Y., Feinberg, M. S., Leor, J., and Cohen, S. (2011). Modulation of cardiac macrophages by phosphatidylserine-presenting liposomes improves infarct repair. *Proc. Natl. Acad. Sci. U. S. A.* 108, 1827–1832. doi:10.1073/pnas.1015623108.
Hayashita, Y., Osada, H., Tatematsu, Y., Yamada, H., Yanagisawa, K., Tomida, S., et al. (2005). A polycistronic MicroRNA cluster, miR-17-92, is overexpressed in human lung cancers and enhances cell proliferation. *Cancer Res.* 65, 9628–9632. doi:10.1158/0008-5472.CAN-05-2352.
Hilfiker-Kleiner, D., Hilfiker, A., Fuchs, M., Kaminski, K., Schaefer, A., Schieffer, B., et al. (2004). Signal transducer and activator of transcription 3 is required for myocardial capillary growth, control of interstitial matrix deposition, and heart protection from ischemic injury. *Circ. Res.* 95, 187–195. doi:10.1161/01.RES.0000134921.50377.61.
Hinkel, R., Penzkofer, D., Zühlke, S., Fischer, A., Husada, W., Xu, Q. F., et al. (2013). Inhibition of microRNA-92a protects against ischemia/reperfusion injury in a large-animal model. *Circulation* 128, 1066–1075. doi:10.1161/CIRCULATIONAHA.113.001904.
Hu, S., Huang, M., Li, Z., and Jia, F. (2011). MicroRNA-210 as a Novel Therapy for Treatment of Ischemic Heart Disease. *Circulation* 122, S124–S131. doi:10.1161/CIRCULATIONAHA.109.928424.MicroRNA-210.
Huang, F., Huang, J.-P., Chen, C., and Chen, M.-H. (2014). Altered microRNAs as novel therapeutic approaches to cardiovascular diseases: an exciting challenge. *Int. J. Cardiol.* 171, e84–5. doi:10.1016/j.ijcard.2013.11.097.
Hughes, J. E., Srinivasan, S., Lynch, K. R., Proia, R. L., Ferdek, P., and Hedrick, C. C. (2008). Sphingosine-1-phosphate induces an antiinflammatory phenotype in macrophages. *Circ. Res.* 102, 950–958. doi:10.1161/CIRCRESAHA.107.170779.
Iaconetti, C., Polimeni, A., Sorrentino, S., Sabatino, J., Pironti, G., Esposito, G., et al. (2012). Inhibition of miR-92a increases endothelial proliferation and migration in

vitro as well as reduces neointimal proliferation in vivo after vascular injury. *Basic Res. Cardiol.* 107. doi:10.1007/s00395-012-0296-y.
Jalil, A., and Seliktar, D. (2015). Hydrogels for therapeutic cardiovascular angiogenesis. *Adv. Drug Deliv. Rev.* 96, 1–9. doi:10.1016/j.addr.2015.07.003.
Jourdan-Lesaux, C., Zhang, J., and Lindsey, M. L. (2010). Extracellular matrix roles during cardiac repair. *Life Sci.* 87, 391–400. doi:10.1016/j.lfs.2010.07.010.
Jung, K., Kim, P., Leuschner, F., Gorbatov, R., Kim, J. K., Ueno, T., et al. (2013). Endoscopic Time-Lapse Imaging of Immune Cells in Infarcted Mouse Hearts. *Circ. Res.* 112, 891–899. doi:10.1161/CIRCRESAHA.111.300484.
Ka, S. O., Song, M. Y., Bae, E. J., and Park, B. H. (2015). Myeloid SIRT1 regulates macrophage infiltration and insulin sensitivity in mice fed a high-fat diet. *J. Endocrinol.* 224, 109–118. doi:10.1530/JOE-14-0527.
Karunakaran, D., Richards, L., Geoffrion, M., Barrette, D., Gotfrit, R. J., Harper, M. E., et al. (2015). Therapeutic Inhibition of miR-33 Promotes Fatty Acid Oxidation but Does Not Ameliorate Metabolic Dysfunction in Diet-Induced Obesity. *Arterioscler. Thromb. Vasc. Biol.* 35, 2536–2543. doi:10.1161/ATVBAHA.115.306404.
Kelly-Laubscher, R. F., King, J. C., Hacking, D., Somers, S., Hastie, S., Stewart, T., et al. (2014). Cardiac preconditioning with sphingosine-1-phosphate requires activation of signal transducer and activator of transcription-3 : cardiovascular topic. *Cardiovasc. J. Afr.* 25, 118–123. doi:10.5830/CVJA-2014-016.
Kempf, T., Zarbock, A., Vestweber, D., and Wollert, K. C. (2012). Anti-inflammatory mechanisms and therapeutic opportunities in myocardial infarct healing. *J. Mol. Med.*, 361–369. doi:10.1007/s00109-011-0847-y.
Kobayashi, H., Minatoguchi, S., Yasuda, S., Bao, N., Kawamura, I., Iwasa, M., et al. (2008). Post-infarct treatment with an erythropoietin-gelatin hydrogel drug delivery system for cardiac repair. *Cardiovasc. Res.* 79, 611–620. doi:10.1093/cvr/cvn154.
Kresh, J. Y., and Chopra, A. (2011). Intercellular and extracellular mechanotransduction in cardiac myocytes. *Pflugers Arch. Eur. J. Physiol.* 462, 75–87. doi:10.1007/s00424-011-0954-1.
Krishnamurthy, P., Rajasingh, J., Lambers, E., Qin, G., Losordo, D. W., and Kishore, R. (2009). IL-10 inhibits inflammation and attenuates left ventricular remodeling after myocardial infarction via activation of STAT3 and suppression of HuR. *Circ. Res.* 104, 9–19. doi:10.1161/CIRCRESAHA.108.188243.
Kukreja, R. C., Yin, C., and Salloum, F. N. (2011). MicroRNAs : New Players in Cardiac Injury and Protection. *Mol. Pharmacol.* 80, 558–564. doi:10.1124/mol.111.073528.tacts.
Kuraitis, D., Ebadi, D., Zhang, P., Rizzuto, E., Vulesevic, B., Padavan, D. T., et al. (2012). Injected matrix stimulates myogenesis and regeneration of mouse skeletal muscle after ischaemic injury. *Eur. Cells Mater.* 24, 175–196.
Kuraitis, D., Hou, C., Zhang, Y., Vulesevic, B., Sofrenovic, T., McKee, D., et al. (2011). Ex vivo generation of a highly potent population of circulating angiogenic cells using a collagen matrix. *J. Mol. Cell. Cardiol.* 51, 187–97. doi:10.1016/j.yjmcc.2011.04.011.
Leonard, B. L., Smaill, B. H., and LeGrice, I. J. (2012). Structural remodeling and mechanical function in heart failure. *Microsc. Microanal.* 18, 50–67. doi:10.1017/S1431927611012438.

Leor, J., Palevski, D., Amit, U., and Konfino, T. (2016). Macrophages and Regeneration: Lessons from the Heart. *Semin. Cell Dev. Biol.* doi:10.1016/j.semcdb.2016.04.012.
Li, A. H., Liu, P. P., Villarreal, F. J., and Garcia, R. a. (2014). Dynamic changes in myocardial matrix and relevance to disease: Translational perspectives. *Circ. Res.* 114, 916–927. doi:10.1161/CIRCRESAHA.114.302819.
Li, L., Wei, W., Zhang, Y., Tu, G., Zhang, Y., Yang, J., et al. (2015). SirT1 and STAT3 protect retinal pigmented epithelium cells against oxidative stress. *Mol. Med. Rep.* 12, 2231–2238. doi:10.3892/mmr.2015.3570.
Li, R., Geng, H., Xiao, J., Qin, X., Wang, F., Xing, J., et al. (2016). miR-7a/b attenuates post-myocardial infarction remodeling and protects H9c2 cardiomyoblast against hypoxia-induced apoptosis involving Sp1 and PARP-1. *Sci. Rep.* 6, 29082. doi:10.1038/srep29082.
Lim, J. P., and Gleeson, P. A. (2011). Macropinocytosis: an endocytic pathway for internalising large gulps. *Immunol. Cell Biol.* 89, 836–843. doi:10.1038/icb.2011.20.
Lin, H.-Y., Chiang, C.-H., and Hung, W.-C. (2013). STAT3 upregulates miR-92a to inhibit RECK expression and to promote invasiveness of lung cancer cells. *Br. J. Cancer* 109, 731–8. doi:10.1038/bjc.2013.349.
Lindsey, M. L., Saucerman, J. J., and DeLeon-Pennell, K. (2016). Knowledge Gaps to Understanding Cardiac Macrophage Polarization Following Myocardial Infarction. *Biochim. Biophys. Acta - Mol. Basis Dis.*, 13–17. doi:10.1016/j.bbadis.2016.05.013.
Mantovani, A., Sica, A., Sozzani, S., Allavena, P., Vecchi, A., and Locati, M. (2004). The chemokine system in diverse forms of macrophage activation and polarization. *Trends Immunol.* 25, 677–86. doi:10.1016/j.it.2004.09.015.
Manukyan, M. C., Alvernaz, C. H., Poynter, J. A., Wang, Y., Brewster, B. D., Weil, B. R., et al. (2011). Interleukin-10 protects the ischemic heart from reperfusion injury via the STAT3 pathway. *Surgery* 150, 231–239. doi:10.1016/j.surg.2011.05.017.
Mcneill, B., Vulesevic, B., Ostojic, A., Ruel, M., and Suuronen, E. J. (2015). Collagen matrix – induced expression of integrin a V b 3 in circulating angiogenic cells can be targeted by matricellular protein CCN1 to enhance their function. *FASEB J.* 29, 1198–1207. doi:10.1096/fj.14-261586.
Nahrendorf, M., Pittet, M. J., and Swirski, F. K. (2010). Monocytes: protagonists of infarct inflammation and repair after myocardial infarction. *Circulation* 121, 2437–45. doi:10.1161/CIRCULATIONAHA.109.916346.
Nahrendorf, M., and Swirski, F. K. (2013). Monocyte and macrophage heterogeneity in the heart. *Circ. Res.* 112, 1624–1633. doi:10.1161/CIRCRESAHA.113.300890.
Nahrendorf, M., Swirski, F. K., Aikawa, E., Stangenberg, L., Wurdinger, T., Figueiredo, J.-L., et al. (2007). The healing myocardium sequentially mobilizes two monocyte subsets with divergent and complementary functions. *J. Exp. Med.* 204, 3037–3047. doi:10.1084/jem.20070885.
Nilsson, S., Möller, C., Jirström, K., Lee, A., Busch, S., Lamb, R., et al. (2012). Downregulation of miR-92a is associated with aggressive breast cancer features and increased tumour macrophage infiltration. *PLoS One* 7. doi:10.1371/journal.pone.0036051.
Nouraee, N., and Mowla, S. J. (2015). miRNA therapeutics in cardiovascular diseases: Promises and problems. *Front. Genet.* 6, 1–6. doi:10.3389/fgene.2015.00232.
O'Connell, R. M., Rao, D. S., Chaudhuri, A. a, and Baltimore, D. (2010). Physiological

and pathological roles for microRNAs in the immune system. *Nat. Rev. Immunol.* 10, 111–22. doi:10.1038/nri2708.

O'Sullivan, K. E., Breen, E. P., Gallagher, H. C., Buggy, D. J., and Hurley, J. P. (2016). Understanding STAT3 signaling in cardiac ischemia. *Basic Res. Cardiol.* 111, 27. doi:10.1007/s00395-016-0543-8.

Okada, H., Lai, N. C., Kawaraguchi, Y., Liao, P., Copps, J., Sugano, Y., et al. (2013). Integrins protect cardiomyocytes from ischemia / reperfusion injury. *J. Clin. Invest.* 123, 4294–4308. doi:10.1172/JCI64216.4294.

Ota, A., Tagawa, H., Karnan, S., Ota, A., Tagawa, H., Karnan, S., et al. (2004). Identification and Characterization of a Novel Gene , C13orf25 , as a Target for 13q31-q32 Amplification in Malignant Lymphoma Identification and Characterization of a Novel Gene , C13orf25 , as a Target for 13q31-q32 Amplification in Malignant Lymphoma. 3087–3095.

Pascual-Gil, S., Garbayo, E., Díaz-Herráez, P., Prosper, F., and Blanco-Prieto, M. J. (2015). Heart regeneration after miocardial infarction using synthetic biomaterials. *J. Control. Release* 203, 23–38. doi:10.1016/j.jconrel.2015.02.009.

Peda, J. K., Salah, S. M., Wallace, D. P., Fields, P. E., Grantham, C. J., Fields, T. A., et al. (2016). Autocrine IL-10 activation of the STAT3 pathway is required for pathogenic macrophage differentiation in polycystic kidney disease. *Dis. Model. Mech.*, dmm.024745. doi:10.1242/dmm.024745.

Pfeffer, M. a, and Braunwald, E. (1990). Ventricular remodeling after myocardial infarction: Experimental observations and clinical implications. *Circulation* 81, 1161–1172. doi:10.1161/01.CIR.81.4.1161.

Piao, H., Kwon, J.-S., Piao, S., Sohn, J.-H., Lee, Y.-S., Bae, J.-W., et al. (2007). Effects of cardiac patches engineered with bone marrow-derived mononuclear cells and PGCL scaffolds in a rat myocardial infarction model. *Biomaterials* 28, 641–9. doi:10.1016/j.biomaterials.2006.09.009.

Pinto, A. R., Godwin, J. W., Chandran, A., Hersey, L., Ilinykh, A., Debuque, R., et al. (2014a). Age-related changes in tissue macrophages precede cardiac functional impairment. *Aging (Albany. NY).* 6, 399–413. Available at: http://www.pubmedcentral.nih.gov/articlerender.fcgi?artid=4069267&tool=pmcentrez&rendertype=abstract.

Pinto, A. R., Godwin, J. W., and Rosenthal, N. a. (2014b). Macrophages in cardiac homeostasis, injury responses and progenitor cell mobilisation. *Stem Cell Res.* 13, 705–714. doi:10.1016/j.scr.2014.06.004.

Pinto, A. R., Paolicelli, R., Salimova, E., Gospocic, J., Slonimsky, E., Bilbao-Cortes, D., et al. (2012). An Abundant Tissue Macrophage Population in the Adult Murine Heart with a Distinct Alternatively-Activated Macrophage Profile. *PLoS One* 7, e36814. doi:10.1371/journal.pone.0036814.

Port, J. D., Walker, L. a, Polk, J., Nunley, K., Buttrick, P. M., and Sucharov, C. C. (2011). Temporal expression of miRNAs and mRNAs in a mouse model of myocardial infarction. *Physiol. Genomics* 43, 1087–95. doi:10.1152/physiolgenomics.00074.2011.

Qin, D., Wang, X., Li, Y., Yang, L., Wang, R., Peng, J., et al. (2016). MiR-223-5p and -3p Cooperatively Suppress Necroptosis in Ischemic/Reperfused Hearts. *J. Biol. Chem.*, jbc.M116.732735. doi:10.1074/jbc.M116.732735.

Raeber, G. P., Lutolf, M. P., and Hubbell, J. a. (2007). Mechanisms of 3-D migration and matrix remodeling of fibroblasts within artificial ECMs. *Acta Biomater.* 3, 615–629. doi:10.1016/j.actbio.2007.03.013.

Rane, A. a, and Christman, K. L. (2011). Biomaterials for the treatment of myocardial infarction: a 5-year update. *J. Am. Coll. Cardiol.* 58, 2615–29. doi:10.1016/j.jacc.2011.11.001.

Ranji, N., Sadeghizadeh, M., Shokrgozar, M. A., Bakhshandeh, B., Karimipour, M., Amanzadeh, A., et al. (2013). MiR-17-92 cluster: an apoptosis inducer or proliferation enhancer. *Mol. Cell. Biochem.* 380, 229–38. doi:10.1007/s11010-013-1678-7.

Rayner, K. J. (2015). MicroRNA-155 in the heart: The right time at the right place in the right cell. *Circulation* 131, 1533–1535. doi:10.1161/CIRCULATIONAHA.115.016327.

Rayner, K. J., Sheedy, F. J., Esau, C. C., Hussain, F. N., Temel, R. E., Parathath, S., et al. (2011). Antagonism of miR-33 in mice promotes reverse cholesterol transport and regression of atherosclerosis. *J. Clin. Invest.* 121, 2921–2931. doi:10.1172/JCI57275.eration.

Rayner, K. J., Suárez, Y., Dávalos, A., Parathath, S., Fitzgerald, M. L., Tamehiro, N., et al. (2010). MiR-33 contributes to the regulation of cholesterol homeostasis. *Science* 328, 1570–3. doi:10.1126/science.1189862.

Rienks, M., Papageorgiou, A.-P., Frangogiannis, N. G., and Heymans, S. (2014). Myocardial extracellular matrix: an ever-changing and diverse entity. *Circ. Res.* 114, 872–88. doi:10.1161/CIRCRESAHA.114.302533.

Ross, R. S., and Borg, T. K. (2001). Integrins and the myocardium. *Circ. Res.* 88, 1112–9. doi:10.1161/hh1101.091862.

Seeger, F. H., Zeiher, A. M., and Dimmeler, S. (2013). MicroRNAs in stem cell function and regenerative therapy of the heart. *Arterioscler. Thromb. Vasc. Biol.* 33, 1739–1746. doi:10.1161/ATVBAHA.113.300138.

Seif-Naraghi, S. B., Singelyn, J. M., Salvatore, M. a, Osborn, K. G., Wang, J. J., Sampat, U., et al. (2013). Safety and efficacy of an injectable extracellular matrix hydrogel for treating myocardial infarction. *Sci. Transl. Med.* 5, 173ra25. doi:10.1126/scitranslmed.3005503.

Serpooshan, V., Zhao, M., Metzler, S. A., Wei, K., Shah, P. B., Wang, A., et al. (2013). The effect of bioengineered acellular collagen patch on cardiac remodeling and ventricular function post myocardial infarction. *Biomaterials* 34, 9048–9055. doi:10.1016/j.biomaterials.2013.08.017.

Shigoka, M., Tsuchida, A., Matsudo, T., Nagakawa, Y., Saito, H., Suzuki, Y., et al. (2010). Deregulation of miR-92a expression is implicated in hepatocellular carcinoma development. *Pathol. Int.* 60, 351–357. doi:10.1111/j.1440-1827.2010.02526.x.

Singelyn, J. M., Sundaramurthy, P., Johnson, T. D., Schup-Magoffin, P. J., Hu, D. P., Faulk, D. M., et al. (2012). Catheter-deliverable hydrogel derived from decellularized ventricular extracellular matrix increases endogenous cardiomyocytes and preserves cardiac function post-myocardial infarction. *J. Am. Coll. Cardiol.* 59, 751–763. doi:10.1016/j.jacc.2011.10.888.

Small, E. M., Frost, R. J. A., and Olson, E. N. (2010). MicroRNAs add a new dimension

to cardiovascular disease. *Circulation* 121, 1022–1032. doi:10.1161/CIRCULATIONAHA.109.889048.

Smart, N., Risebro, C. a, Melville, A. a D., Moses, K., Schwartz, R. J., Chien, K. R., et al. (2007). Thymosin beta4 induces adult epicardial progenitor mobilization and neovascularization. *Nature* 445, 177–182. doi:10.1038/nature05383.

Somers, S. J., Frias, M., Lacerda, L., Opie, L. H., and Lecour, S. (2012). Interplay between SAFE and RISK pathways in sphingosine-1-phosphate-induced cardioprotection. *Cardiovasc. Drugs Ther.* 26, 227–237. doi:10.1007/s10557-012-6376-2.

Steg, P. G., James, S. K., Atar, D., Badano, L. P., Lundqvist, C. B., Borger, M. A., et al. (2012). ESC Guidelines for the management of acute myocardial infarction in patients presenting with ST-segment elevation: The Task Force on the management of ST-segment elevation acute myocardial infarction of the European Society of Cardiology (ESC). *Eur. Heart J.* 33, 2569–2619. doi:10.1093/eurheartj/ehs215.

Sutton, M. G. S. J., and Sharpe, N. (2015). Left Ventricular Remodeling After Myocardial Infarction Pathophysiology and Therapy. *Circulation* 101, 2981–2988.

Suuronen, E. J., Veinot, J. P., Wong, S., Kapila, V., Price, J., Griffith, M., et al. (2006). Tissue-engineered injectable collagen-based matrices for improved cell delivery and vascularization of ischemic tissue using CD133+ progenitors expanded from the peripheral blood. *Circulation* 114, I138–44. doi:10.1161/CIRCULATIONAHA.105.001081.

Suuronen, E. J., Zhang, P., Kuraitis, D., Cao, X., Melhuish, A., McKee, D., et al. (2009). An acellular matrix-bound ligand enhances the mobilization, recruitment and therapeutic effects of circulating progenitor cells in a hindlimb ischemia model. *FASEB J.* 23, 1447–58. doi:10.1096/fj.08-111054.

Swirski, F. K., and Nahrendorf, M. (2013). Leukocyte Behavior in Atherosclerosis, Myocardial Infarction, and Heart Failure. *Science (80-.).* 161, 161–166. doi:10.1126/science.1230719.

Swirski, F. K., Nahrendorf, M., Etzrodt, M., Wildgruber, M., Panizzi, P., Figueiredo, J., et al. (2009). Identification Monocytes Inflammatory of Splenic Reservoir and Their Deployment Sites. *Science (80-.).* 325, 612–616. doi:10.1126/science.1175202.Identification.

Tallawi, M., Rosellini, E., Barbani, N., Cascone, M. G., Rai, R., Saint-Pierre, G., et al. (2015). Strategies for the chemical and biological functionalization of scaffolds for cardiac tissue engineering: a review. *Interface* 12, 20150254. doi:10.1098/rsif.2015.0254.

Toeg, H. D., Tiwari-Pandey, R., Seymour, R., Ahmadi, A., Crowe, S., Vulesevic, B., et al. (2013). Injectable small intestine submucosal extracellular matrix in an acute myocardial infarction model. *Ann. Thorac. Surg.* 96, 1686–94; discussion 1694. doi:10.1016/j.athoracsur.2013.06.063.

Venugopal, J. R., Prabhakaran, M. P., Mukherjee, S., Ravichandran, R., Dan, K., and Ramakrishna, S. (2012). Biomaterial strategies for alleviation of myocardial infarction. *J. R. Soc. Interface* 9, 1–19. doi:10.1098/rsif.2011.0301.

Wang, R. M., and Christman, K. L. (2015). Decellularized myocardial matrix hydrogels: In basic research and preclinical studies. *Adv. Drug Deliv. Rev.* 96, 77–82. doi:10.1016/j.addr.2015.06.002.

Wang, Y., Dongfei, W., Zhang, L., Ye, F., Li, M., and Wen (2016). Role of JAK-STAT pathway in reducing cardiomyocytes hypoxia/ reoxygenation injury induced by S1P postconditioning. *Eur. J. od Pharmacol.* 784, 181–185. doi:10.1016/j.ejphar.2016.05.024.

Wang, Z., Cui, Y., Wang, J., Yang, X., Wu, Y., Wang, K., et al. (2014). The effect of thick fibers and large pores of electrospun poly(ε-caprolactone) vascular grafts on macrophage polarization and arterial regeneration. *Biomaterials* 35, 5700–5710. doi:10.1016/j.biomaterials.2014.03.078.

Wijns, W., Kolh, P., Danchin, N., Di Mario, C., Falk, V., Folliguet, T., et al. (2010). Guidelines on myocardial revascularization: The Task Force on Myocardial Revascularization of the European Society of Cardiology (ESC) and the European Association for Cardio-Thoracic Surgery (EACTS). *Eur. Heart J.* 31, 2501–2555. doi:10.1093/eurheartj/ehq277.

Winslow, R. L., Walker, M. A., and Greenstein, J. L. (2015). Modeling calcium regulation of contraction, energetics, signaling, and transcription in the cardiac myocyte. *Wiley Interdiscip. Rev. Syst. Biol. Med.* 8, n/a–n/a. doi:10.1002/wsbm.1322.

Wynn, T. A., and Vannella, K. M. (2016). Macrophages in Tissue Repair, Regeneration, and Fibrosis. *Immunity* 44, 450–462. doi:10.1016/j.immuni.2016.02.015.

Xu, G., Wang, X., Deng, C., Teng, X., Suuronen, E. J., Shen, Z., et al. (2014). Injectable biodegradable hybrid hydrogels based on thiolated collagen and oligo(acryloyl carbonate)-poly(ethylene glycol)-oligo(acryloyl carbonate) copolymer for functional cardiac regeneration. *Acta Biomater.* 15, 55–64. doi:10.1016/j.actbio.2014.12.016.

Yan, X., Anzai, A., Katsumata, Y., Matsuhashi, T., Ito, K., Endo, J., et al. (2013). Temporal dynamics of cardiac immune cell accumulation following acute myocardial infarction. *J. Mol. Cell. Cardiol.* 62, 24–35. doi:10.1016/j.yjmcc.2013.04.023.

Yoshizaki, T., Schenk, S., Imamura, T., Babendure, J. L., Sonoda, N., Bae, E. J., et al. (2010). SIRT1 inhibits inflammatory pathways in macrophages and modulates insulin sensitivity. *Am. J. Physiol. Endocrinol. Metab.* 298, E419–E428. doi:10.1152/ajpendo.00417.2009.

Zhang, B., Zhou, M., Li, C., Zhou, J., Li, H., Zhu, D., et al. (2014). MicroRNA-92a inhibition attenuates hypoxia/reoxygenation-induced myocardiocyte apoptosis by targeting Smad7. *PLoS One* 9, 5–12. doi:10.1371/journal.pone.0100298.

Zhang, L., and Wang, C.-C. (2014). Inflammatory response of macrophages in infection. *Hepatobiliary Pancreat. Dis. Int.* 13, 138–152. doi:10.1016/S1499-3872(14)60024-2.